

Textual Planning with Explicit Latent Transitions

Eliezer Shlomi^{*1} Ido Levy^{*2} Eilam Shapira¹ Michael Katz² Guy Uziel² Segev Shlomov² Nir Mashkif²
Roi Reichart¹ Sarah Keren¹

Abstract

Planning with LLMs is bottlenecked by token-by-token generation and repeated full forward passes, making multi-step lookahead and rollout-based search expensive in latency and compute. We propose EMBEDPLAN, which replaces autoregressive next-state generation with a lightweight transition model operating in a frozen language embedding space. EmbedPlan encodes natural language state and action descriptions into vectors, predicts the next-state embedding, and retrieves the next state by nearest-neighbor similarity, enabling fast planning computation without finetuning the encoder. We evaluate the next state prediction across 9 classical planning domains using six evaluation protocols of increasing difficulty: Interpolation, Plan-Variant, Extrapolation, Multi-Domain, Cross-Domain, and Leave-One-Out. Results show near-perfect interpolation performance but a sharp degradation when generalization requires transfer to unseen problems or unseen domains; Plan-Variant evaluation indicates generalization to alternative plans rather than memorizing seen trajectories. Overall, frozen embeddings support within-domain dynamics learning after observing a domain’s transitions, while transfer across domain boundaries remains a bottleneck.

1. Introduction

Planning with large language models requires generating action sequences token-by-token, invoking full forward passes per decision. This makes multi-step lookahead and rollout-based search, essential for robust, long-horizon planning, prohibitively expensive in latency and cost. The bottleneck is fundamental: without a compact transition function that predicts how actions transform states, planners cannot

^{*}Equal contribution ¹Technion – Israel Institute of Technology, Haifa, Israel ²IBM, Haifa, Israel. Correspondence to: Eliezer Shlomi <Eliezer@campus.technion.ac.il>, Ido Levy <Ido.Levy1@ibm.com>.

cheaply evaluate alternatives or backtrack from errors.

Although efforts have addressed this via prompting-based reasoning (Wei et al., 2022; Yao et al., 2023; 2022), symbolic compilation to Planning Domain Definition Language (PDDL) (Liu et al., 2023; Guan et al., 2023; Oswald et al., 2024; Tantakoun et al., 2025; Zuo et al., 2025), and end-to-end latent world models (Ha & Schmidhuber, 2018; Hafner et al., 2020; Schriftwieser et al., 2020), a key opportunity remains: can we leverage pre-trained language embeddings to construct efficient transition functions? Replacing autoregressive generation with lightweight operations in a frozen embedding space offers an architectural path toward reduced planning computation at inference time.

We introduce **EMBEDPLAN**, a framework that learns explicit transition dynamics directly in frozen LLM embedding space over text-described planning domains. Rather than generating next states autoregressively, EMBEDPLAN encodes natural language state descriptions (e.g., “Block A is on B, Block C is clear”) and action descriptions (e.g., pick-up (C)) into vectors, trains a lightweight network (<500K parameters) to predict next-state embeddings, and retrieves candidates by cosine similarity (Figure 1). EMBEDPLAN training combines two contrastive objectives: state prediction, which learns to identify correct next states among candidates, and action disambiguation, which learns to distinguish the effects of different actions applied to the same state. Together, these losses enable both accurate retrieval and fine-grained action semantics. This architecture decouples semantic understanding, handled by frozen pre-trained language encoders, from dynamics prediction, handled by learned transition networks, collapsing the need of expensive LLM calls into cheap embedding space operations while enabling modular updates and test-time verification. We isolate and characterize what frozen pretrained embeddings can support for transition learning, independent of search algorithms or symbolic compilation. We hypothesize that LLM embeddings encode sufficient structural regularities to support generalizable transition learning when planning problems are rendered as natural language.

We evaluate the next state prediction ability of EMBEDPLAN across 9 classical planning domains from ACP-BENCH (Kokel et al., 2025a), each rendered as natural

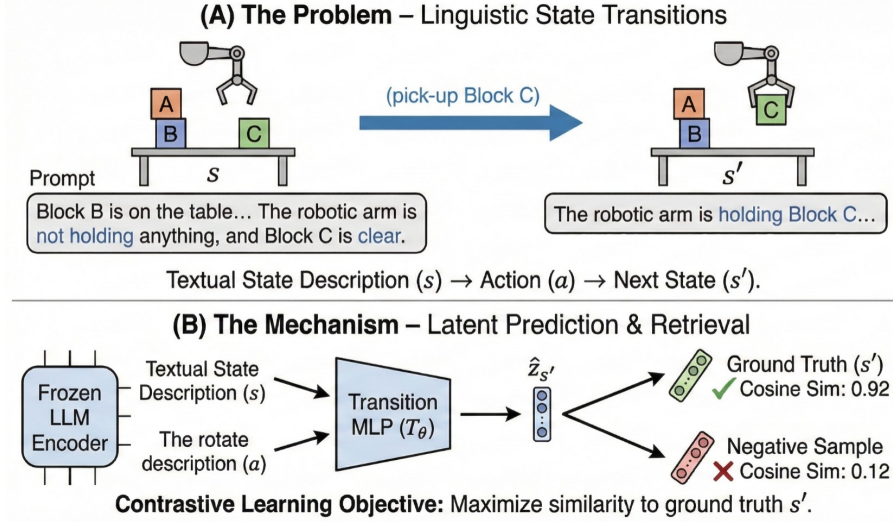


Figure 1. EMBEDPLAN: Latent Transition Learning. (A) Planning domains define state transitions as linguistic triplets (s, a, s') : the Blocksworld action `pick-up` (C) transforms the textual state description from “arm is empty, C is clear” to “arm is holding C.” (B) EMBEDPLAN encodes states and actions via frozen LLM embeddings, then trains a lightweight transition network T_θ to predict next-state embeddings. Contrastive learning (InfoNCE) pulls predictions toward ground-truth states while pushing away negatives; inference retrieves the nearest candidate.

language state descriptions within a cumulative dataset of over 3 million transitions, using six protocols: Interpolation split (interpolation within problem manifolds), Extrapolation split (extrapolation to new problems), Cross-Domain transfer, Multi-Domain learning, and Leave-One-Out generalization. We compare Llama-3.3-70B (4096-dim) and all-mpnet-base-v2 (768-dim) sentence embeddings, measuring next-state retrieval accuracy (Hit@ k) across all conditions.

Our experiments reveal a sharp capability boundary for latent transition learning in frozen embedding spaces. Within known problem manifolds, EMBEDPLAN achieves near-perfect next-state retrieval (99.7% Hit@5 under Interpolation), showing that pretrained embeddings are sufficient for learning accurate dynamics when train and test share the same underlying instances. However, this ability degrades substantially when generalization requires structural transfer: performance drops to 54.6% on unseen problem configurations (Extrapolation; a 45.2 pp gap), and transfer across domain boundaries fails, with Cross-Domain reaching only 6.6% Hit@5 (+2.7 pp above the 3.9% untrained baseline) and Leave-One-Out achieving just 9.2% on the held-out ninth domain. Importantly, the within-domain generalization is not explained by memorizing training-set plans: in the Plan-Variant setting, where test problems require executing alternative optimal solution paths for the same underlying instances, EMBEDPLAN still achieves 51.2% mean complete plan execution, indicating that it learns reusable action-conditioned dynamics rather than merely replaying trajectories. Together, these results confirm that frozen embeddings support generalization primarily after exposure to

the target domain’s dynamics, enabling meaningful extrapolation within a domain once its transition structure has been observed. Despite these limitations, we find two positive signals for practitioners: (i) joint training across all 9 domains retains meaningful performance (37.2% Hit@5) without catastrophic forgetting, and (ii) larger encoders consistently improve learnability (up to +104%).

We make key three contributions:

1. We introduce EMBEDPLAN, a novel application of learning action-conditioned transitions in frozen LLM embedding spaces without encoder finetuning.
2. We rigorously characterize generalization boundaries via controlled protocols (interpolation, plan variation, extrapolation, and transfer), establishing a reusable evaluation methodology for latent dynamics models.
3. We establish a six-protocol hierarchy across 9 domains and 4 encoders for standardized evaluation.

2. Related Work

Prompting-based reasoning methods framed planning as iterative generation over intermediate thoughts. Wei et al. (2022) showed that chain-of-thought prompting elicits multi-step rationales from large models, and building on this idea, Yao et al. (2023) proposed tree search over candidate reasoning trajectories. Action-grounded schemes interleave reasoning with environment interaction, with ReAct-style traces enabling agents to update beliefs from observations (Yao et al., 2022; Shinn et al., 2023). More explicit planning formulations treat the LLM as a world model combined with

Monte Carlo Tree Search (Hao et al., 2023), while complementary work compiles natural language goals into PDDL and invokes classical solvers (Liu et al., 2023; Guan et al., 2023). However, these approaches rely on repeated LLM calls per decision, and recent critiques emphasize brittleness, hallucinated actions, and mismatches between generated rationales and executable plans (Kambhampati et al., 2024; Katz et al., 2024). EMBEDPLAN addresses this bottleneck by testing whether next state can be computed efficiently in a frozen embedding space using latent transition function.

Early work demonstrated that planning can be done in the learned latent space rather than in the hand-crafted symbolic state space. Asai & Fukunaga (2018) introduced LATPLAN, which learns discrete state encodings from visual inputs via autoencoders and applies classical planners in latent space. Model-based reinforcement learning extended this by learning dynamics models that predict latent states under actions (Ha & Schmidhuber, 2018; Hafner et al., 2019; 2020; Schrittwieser et al., 2020). Recently, Micheli et al. (2023) applied transformer architectures to world modeling with high sample efficiency on Atari, while Gieselmann & Pokorny (2022) developed Expansive Latent Space Trees (ELAST) for tree search over visual dynamics. However, these methods operate in visual domains with limited action primitives. To our knowledge, our work is the first to translate this paradigm to natural language, where the transition function must generalize across combinatorial textual action spaces rather than fixed motor primitives. Unlike end-to-end training, EMBEDPLAN operates with frozen LLM embeddings and evaluates whether learned transition functions support multi-step planning across 9 classical domains, quantifying within-distribution success and out-of-distribution collapse. Object-centric architectures that factor states into entities and relations (Battaglia et al., 2018) and symbolic compilation to PDDL (Liu et al., 2023; Guan et al., 2023) offer complementary inductive biases for cross-domain transfer; our study establishes the baseline capability of unstructured text embeddings, quantifying the gap that structured approaches must close and providing a diagnostic methodology against which such methods can be measured.

Sentence embedding methods target semantic similarity, often using contrastive objectives (Reimers & Gurevych, 2019; Gao et al., 2021; Radford et al., 2021; Oved et al., 2025). Representation learning for control leverages similar contrastive signals to induce state structure (Oord et al., 2018; Laskin et al., 2020; Schwarzer et al., 2021), while JEPA-style methods predict held-out representations in an embedding space rather than reconstructing raw inputs (Assran et al., 2023). Retrieval-augmented models similarly rely on embedding space lookups for prediction (Khandelwal et al., 2020) and control (Humphreys et al., 2022). However, these approaches largely focus on visual/RL settings or general-purpose similarity, and are not evaluated as action-

conditioned transition operators for planning in frozen language embedding spaces. EMBEDPLAN bridges this gap by learning transition functions in a frozen LLM embedding space and systematically evaluating generalization across planning domains and problem configurations.

Classical planning benchmarks provide controlled testbeds (McDermott et al., 1998). ACPBENCH measures predictive transition accuracy and generalization across held-out problems (Kokel et al., 2025a). A recent extension, (Kokel et al., 2025b), introduces open-ended generative versions of these tasks. Compositional generalization benchmarks reveal that neural models often memorize training patterns (Lake & Baroni, 2018; Kim & Linzen, 2020). EMBEDPLAN evaluates transition learning in embedding space with explicit within-distribution and out-of-distribution metrics, connecting failures to embedding clustering by problem instance rather than generalizable structure.

3. Experimental Setup

Task Formulation. Given a state s and action a described in natural language, we aim to predict the next state s' . Let $E : \mathcal{S} \rightarrow \mathbb{R}^d$ denote a frozen LLM encoder mapping text to embeddings. We train a lightweight transition network $T_\theta : \mathbb{R}^d \times \mathbb{R}^d \rightarrow \mathbb{R}^d$ to predict the next-state embedding:

$$\hat{\mathbf{e}}_{s'} = T_\theta(E(s), E(a)) \quad (1)$$

At inference, we retrieve the next state by finding the nearest neighbor in a candidate pool \mathcal{C} of encoded states:

$$\hat{s}' = \arg \max_{s' \in \mathcal{C}} \text{sim}(\hat{\mathbf{e}}_{s'}, E(s')) \quad (2)$$

where $\text{sim}(\cdot, \cdot)$ denotes cosine similarity. This retrieval formulation assumes access to a candidate pool, appropriate for settings with enumerable state spaces (classical planning benchmarks, model-based RL with discrete observations).

Data. We construct transition datasets from 9 classical PDDL planning domains sourced from ACPBENCH (Kokel et al., 2025a): Blocksworld, Depot, Ferry, Floortile, Goldminer, Grid, Logistics, Rovers, and Satellite. These span manipulation, logistics, and navigation tasks with varying structural complexity. Each domain contains multiple problem instances: specific configurations of objects, initial states, and goals (e.g., a particular arrangement of blocks to be stacked into a target configuration). For each problem, we obtain one or more optimal plans (up to 100 per problem): trajectories of states connected by actions, $\tau = (s_1, a_1, s_2, a_2, \dots, a_{n-1}, s_n)$, where each action a_t transforms state s_t into successor state s_{t+1} . From these trajectories, we extract state-action-next-state triplets (s_t, a_t, s_{t+1}) as training examples. The dataset comprises 2,969,574 transitions across 67 problems (259,427 states),

with per-domain counts ranging from 13,256 (Depot) to 1,248,696 (Satellite). More details in Appendix C.

Architecture. Our model (Figure 1) comprises: (1) frozen encoder producing state and action embeddings, (2) learned projection heads reducing dimensionality to 128, and (3) a transition network predicting the next-state embedding. We evaluate two transition architectures: a residual MLP that concatenates inputs and adds a skip connection, and a hypernetwork that generates action-specific transformation parameters. Both are lightweight (<500K trainable parameters). The residual MLP consistently outperforms the hypernetwork across encoders and protocols (Appendix G.1), so we report MLP results throughout the paper. Full architectural details appear in Appendix B.1 (Figure 4).

Training Objective. We train with a composite contrastive objective:

$$\mathcal{L} = \mathcal{L}_{\text{state}} + \lambda \cdot \mathcal{L}_{\text{action}} \quad (3)$$

where λ controls action disambiguation emphasis.

The **state prediction loss** $\mathcal{L}_{\text{state}}$ is InfoNCE (Oord et al., 2018) over next-state candidates: given a batch of B transitions, it pulls predicted embeddings toward ground-truth next states while pushing away other batch states. This teaches the model which state results from a transition, capturing coarse domain dynamics.

The **action disambiguation loss** $\mathcal{L}_{\text{action}}$ distinguishes effects of different actions applied to the same state. For each transition (s, a, s') , we apply K applicable ground actions to s and ensure the prediction from the correct action a is closest to ground-truth s' . Here K denotes fully instantiated actions (e.g., pick-up (BlockA)); for large action sets, we sample up to $K=50$. This teaches fine-grained action semantics critical for planning. Full formulations appear in Appendix B.2.

We set $\lambda = 2$ after grid search (Appendix B.2.3), emphasizing action disambiguation (ablation in Appendix G.2). Training uses batch size 128, temperature $\tau = 0.07$, AdamW with learning rate 4×10^{-5} , and early stopping. Training completes in ~ 2 hours per domain on a single A100.

Evaluation Protocols. We evaluate on six protocols that measure increasingly demanding generalization capabilities (definitions in Appendix A):

- **Interpolation split:** Transitions randomly assigned to train (80%) and test (20%). The same problem instance may contribute to both sets. This measures interpolation within known problem manifolds.
- **Plan-Variant split:** Evaluate full-plan execution on alternative optimal plans for problems seen during train-

ing. Train and test share the same underlying problem instances, but differ in the action sequences used to reach the goal. This measures generalization to unseen solution paths under fixed problem structure.

- **Extrapolation split:** Entire problems assigned to train or test. All transitions from held-out problems are unseen during training. This measures extrapolation to new problem configurations within a known domain.
- **Cross-Domain transfer:** Train on one source domain, evaluate on a different target domain with no shared problems or domain structure. This measures zero-shot domain transfer.
- **Multi-Domain learning:** Train a single unified model on all 9 domains simultaneously, evaluate on held-out problems from each domain (Problem-Grouped within each). This measures whether a shared transition network can serve multiple domains without catastrophic forgetting.
- **Leave-One-Out (LOO) generalization:** Train on 8 domains, evaluate on the held-out 9th domain. Measures whether exposure to diverse domains enables transfer to an unseen domain.

Metrics. We report Hit@ k ($k \in \{1, 5, 10\}$): the proportion of queries where the correct next state ranks within the top- k retrieved candidates. The candidate pool contains 128 states: the ground-truth next state with 127 distractors. This controlled retrieval setting enables precise measurement of discriminative capability; practical deployment would require either pre-enumerated state spaces or generative mechanisms to produce candidates extensions we identify as future work. Under Interpolation, distractors are sampled uniformly from all domain states. Under Extrapolation, distractors are sampled exclusively from the same problem instance as the query state, ensuring that all candidates share the same object vocabulary and structural context. This design makes Extrapolation strictly harder: the model must distinguish among states within a single problem’s manifold rather than across heterogeneous configurations. An untrained model with random weights (Appendix D.6) establishes chance-level performance as a lower bound for comparison.

We emphasize Hit@5 for two reasons. First, multiple optimal plans exist per problem, so Hit@1 can penalize predictions that correspond to alternative valid trajectories rather than genuine errors. Second, our lightweight architecture naturally enables beam search over multiple candidate futures at inference time, where ensuring the ground truth ranks within the beam matters more than perfect top-1 accuracy. We report Hit@1 throughout for completeness.

Table 1. Encoder Comparison. Hit@5 (%) for interpolation and extrapolation. Extrapolation varies by $2\times$ across encoders. Gap significance: *** $p<0.001$, ** $p<0.01$ (paired t -test, $n=9$ domains). Full statistical analysis including effect sizes appears in Appendix E.

Encoder	Dim	Interp.	Extrap.	Gap
MPNet	768	70.0 \pm 44	26.8 \pm 19	43**
BGE-M3	1,024	99.6 \pm 0.5	36.3 \pm 15	63***
Qwen2.5-7B	3,584	99.5 \pm 0.6	47.7 \pm 15	52***
Llama-3.3-70B	8,192	99.7 \pm 0.4	54.6 \pm 17	45***

4. Results

We evaluate whether frozen LLM embeddings support generalizable transition learning. Results report the best configuration, averaged over 3 seeds. More details in Appendix D.

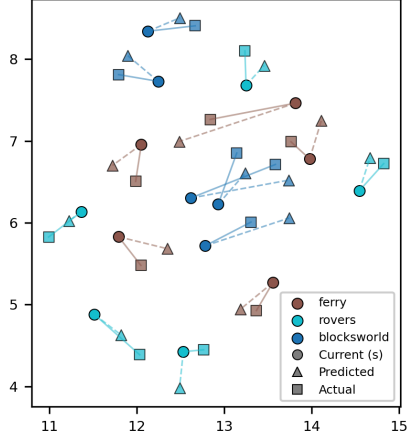


Figure 2. PCA of sampled transitions from three domains. States s (○), predictions \hat{s}' (\triangle), and ground-truth s' (\square); dashed lines link each prediction to its source state. Interpolation, BGE-M3.

Transition Learning with Frozen Embeddings We evaluate two generalization settings: *interpolation* (Interpolation split, predicting held-out steps from partially observed problems) and *extrapolation* (Extrapolation split, generalizing to entirely unseen problem configurations). Table 1 presents results for four encoder sizes (Appendix B.1.1).

Under the Interpolation split, analogous to masked language modeling where the model predicts held-out planning steps from partially observed problems, models with expressive embeddings achieve near-perfect performance: Llama-3.3-70B attains 99.7% Hit@5. This establishes that frozen LLM embeddings encode sufficient structure to support dynamics learning without task-specific fine-tuning. Visualizations of

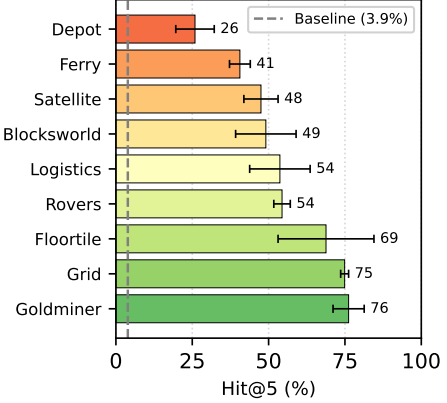


Figure 3. Extrapolation by Domain (Llama-3.3-70B). Hit@5 (%) under Problem-Grouped evaluation. Dashed line: untrained baseline (3.9%). Error bars: \pm SE.

learned transitions confirm this finding: as shown in Figure 2, predicted next-state embeddings consistently land near ground-truth embeddings in PCA projections, demonstrating that the transition network learns accurate displacement vectors in the latent space.

Under Extrapolation evaluation, Llama-3.3-70B achieves 54.6%, a 45 pp decline from interpolation but still 14 \times above the 3.9% untrained baseline. This substantial improvement over chance indicates that models learn transferable domain structure, not merely problem-specific memorization. However, the consistent gap across encoders reveals that roughly half of predictive capability relies on problem-specific patterns that do not transfer to novel configurations. This gap is amplified by our evaluation design: Extrapolation distractors come from the same problem instance, forcing discrimination among structurally similar configurations. Scaling embedding dimension improves extrapolation, from 26.8% (MPNet, 768-d) to 54.6% (Llama-3.3-70B, 8,192-d), with diminishing returns: the gain from Qwen2.5-7B to Llama-3.3-70B (+6.9 pp) is smaller than earlier scaling steps, suggesting a plateau larger embeddings cannot bridge.

Figure 3 shows extrapolation varies substantially across domains (26%–76%). Complete per-domain results appear in Table 8. Grid-based domains with predictable spatial dynamics (Goldminer, Grid) generalize best; domains requiring compositional multi-object reasoning (Depot) show larger gaps. This pattern suggests that the domain structure, not the scale, determines the difficulty of generalization. We attribute this to embeddings encoding semantic similarity rather than structural equivalence: the model cannot recognize that “pick-up(BlockA)” and “board(Car1)” share the same abstract precondition-effect schema, as LLM embeddings cluster states by lexical surface form rather than the structural role in planning (Appendix F.1).

Table 2. Single-Step Transition Prediction (Interpolation Split, Llama-3.3-70B). *Next State Prediction*: whether the ground-truth next state is in top- k retrieved candidates. *Action Disambiguation*: whether, among all actions applied to s , the correct action a produces the prediction closest to ground-truth s' . High Acc@5 (85.3%) confirms the model captures action-specific transformation patterns.

Domain	Next State Prediction (%)			Action Disambiguation (%)		
	Hit@1	Hit@5	Hit@10	Acc@1	Acc@5	Acc@10
Blocksworld	94.6 \pm 0.4	100.0 \pm 0.0	100.0 \pm 0.0	25.9 \pm 0.9	88.6 \pm 0.2	99.5 \pm 0.1
Depot	76.9 \pm 1.2	98.8 \pm 0.1	99.4 \pm 0.1	29.8 \pm 2.3	82.2 \pm 2.1	93.3 \pm 1.4
Ferry	98.5 \pm 0.2	100.0 \pm 0.0	100.0 \pm 0.0	43.1 \pm 0.8	96.8 \pm 0.1	99.8 \pm 0.0
Floortile	97.9 \pm 0.4	99.6 \pm 0.0	99.8 \pm 0.0	37.1 \pm 2.8	86.5 \pm 1.9	97.3 \pm 0.8
Goldminer	93.8 \pm 0.8	100.0 \pm 0.0	100.0 \pm 0.0	17.0 \pm 0.5	73.3 \pm 0.6	97.4 \pm 0.2
Grid	90.1 \pm 0.2	99.8 \pm 0.1	99.9 \pm 0.0	28.6 \pm 0.2	86.7 \pm 0.1	96.4 \pm 0.3
Logistics	93.4 \pm 0.6	99.9 \pm 0.1	99.9 \pm 0.0	25.1 \pm 2.0	81.3 \pm 3.8	94.0 \pm 1.9
Rovers	86.0 \pm 0.8	99.0 \pm 0.1	99.6 \pm 0.1	26.1 \pm 1.5	73.9 \pm 1.4	86.3 \pm 0.7
Satellite	97.6 \pm 0.2	99.9 \pm 0.0	100.0 \pm 0.0	55.0 \pm 1.7	98.5 \pm 0.3	99.9 \pm 0.0
Mean	92.1 \pm 6.5	99.7 \pm 0.4	99.8 \pm 0.2	32.0 \pm 11.4	85.3 \pm 8.3	96.0 \pm 4.1

Single-Step Prediction and Action Disambiguation Table 2 provides a detailed per-domain breakdown of single-step transition prediction under the Interpolation split, reporting Hit@ k for $k \in \{1, 5, 10\}$. The results confirm consistent interpolation success across all nine domains, with Hit@5 exceeding 98.8% in every case. Hit@1 performance is similarly strong (mean 92.1%), though Depot emerges as an outlier with the lowest Hit@1 (76.9%). Notably, this same domain exhibits the weakest extrapolation performance (26%), suggesting that Depot’s complex multi-object interactions pose semantic state representation challenges even within known (trained) problem manifolds.

Beyond next-state prediction, we evaluate whether the transition network captures fine-grained action semantics through an action disambiguation task. For each test transition (s, a, s') , we apply all possible actions to state s , producing a set of candidate next-state predictions $\{\hat{s}'_{a_1}, \dots, \hat{s}'_{a_k}\}$ where each prediction corresponds to a different action. We then check whether the ground-truth next state s' is closest to the prediction from the correct action a , rather than to predictions from distractor actions. This tests whether the model distinguishes the causal effect of the applied action from plausible alternatives, validating that our transition model understands action-space implications when faced with fine-grained distractors.

Action disambiguation achieves strong performance: mean Acc@5 reaches 85.3%, indicating the model correctly identifies the applied action among the top-5 candidates in most cases. This confirms that the transition network learns action-specific transformation patterns, not merely generic state-to-state mappings. Notably, Satellite achieves 98.5% Acc@5 while Goldminer shows lower action accuracy (73.3%), suggesting that some domains have more distinguishable action effects than others. The gap between Hit@1 (92.1%) and Acc@1 (32.0%) reveals that while the model reliably predicts correct next states, pinpointing the

exact action among fine-grained alternatives remains challenging at strict thresholds. Qualitative error analysis reveals that incorrect retrievals often share the query’s problem instance and differ by one or two predicates, suggesting the model captures coarse dynamics but struggles with fine-grained predicate-level precision (examples in Appendix J).

Full Plan Execution The single-step results above evaluate isolated transitions. To assess multi-step reliability, we evaluate full plan execution under teacher forcing, intentionally isolating transition quality from error accumulation dynamics to enable clean capability measurement. Given an optimal plan $\pi = (a_1, \dots, a_n)$ for a problem, we iterate from s_0 and, at each step t , retrieve the top- k successor candidates for (s_{t-1}, a_t) and record whether the ground-truth successor s_t appears in the top- k (Hit@ k). We then feed the ground-truth s_t as input to the next step. Teacher forcing decouples transition quality from compounding state-distribution drift, so this measures whether the correct successor stays within the retrieval beam throughout the plan.

Table 3. Plan-Variant Split Evaluation, Llama-3.3-70B. Mean and exact plan execution under Hit@5.

Domain	Mean	Exact
Blocksworld	38.7 \pm 0.8	1.6 \pm 0.2
Depot	30.1 \pm 2.6	11.2 \pm 1.5
Ferry	71.1 \pm 1.1	39.1 \pm 1.6
Floortile	74.1 \pm 2.7	33.6 \pm 3.3
Goldminer	55.4 \pm 2.2	23.8 \pm 1.6
Grid	55.0 \pm 2.4	37.4 \pm 2.2
Logistics	52.8 \pm 0.6	14.1 \pm 2.0
Rovers	26.5 \pm 0.8	10.0 \pm 0.7
Satellite	56.8 \pm 1.2	32.2 \pm 1.0
Mean	51.2 \pm 16.6	22.6 \pm 13.7

This evaluation introduces a subtle generalization challenge

that we term the Plan-Variant split. We test on alternative optimal plans for problems seen during training: since multiple optimal solutions may exist for the same problem, train and test trajectories can differ even when derived from the same underlying instance. The model thus encounters novel action sequences not observed during training, testing latent planning generalization across equivalent solution paths.

Table 3 reports plan-level performance under two metrics. *Mean* measures the average per-step Hit@5 across the plan, while *Exact* requires *every* step to succeed (a single failure yields 0). The gap between Mean (51.2%) and Exact (22.6%) reflects compounding errors over multi-step rollouts: even moderate per-step failure rates accumulate to substantially reduce whole-plan success.

Performance varies markedly by domain. Ferry and Floor-tile achieve the highest Exact rates (39.1% and 33.6%), while Blocksworld collapses to 1.6% Exact despite reasonable Mean (38.7%). We attribute this sensitivity to two factors: (1) state similarity, as domains like Blocksworld contain many near-identical configurations differing only in object arrangements, making disambiguation difficult; and (2) sparse coverage of critical transitions, it possible that certain planning phases (e.g., intermediate stack configurations) may be underrepresented in training trajectories, causing failures precisely where precision matters most. Crucially, the Plan-Variant split tests on alternative optimal plans for training problems, action sequences the model never observed. That Mean remains above 50% under this condition provides evidence against pure trajectory memorization: the model captures transferable transition dynamics rather than simply replaying seen action sequences. The gap between Mean (51.2%) and Exact (22.6%) quantifies potential error accumulation: even without closed-loop compounding, moderate per-step failures substantially reduce whole-plan success, indicating that deployment in planning systems would require error recovery mechanisms. Plan-level results for other encoders appear in Appendix D.7.

Transfer Across Domain Boundaries Established within-domain learning potential, we ask whether learned dynamics transfer across domains. Table 4 presents a generalization hierarchy spanning chance-level to near-perfect performance.

Zero-shot transfer fails almost completely. Cross-Domain achieves only 6.6%, merely +2.7 pp above chance. The complete 9×9 transfer matrix (Table 10) reveals that the only notable success is Ferry \rightarrow Logistics (22.3%), attributable to shared transportation semantics in their state descriptions. Leave-One-Out fares little better at 9.2% despite training on eight related domains (Table 11). This failure underscores a fundamental limitation: although all PDDL domains share discrete state spaces, typed objects, and precondition-effect schemas, latent planners trained on

Table 4. Generalization Hierarchy. Hit@5 (%) across protocols of increasing difficulty. Cross-Domain and LOO barely exceed the 3.9% baseline, indicating near-zero transfer. Per-protocol breakdowns in Appendix D.

Protocol	Hit@5	Δ	Setting
Untrained	3.9 \pm 0.1	—	Chance
Cross-Domain	6.6 \pm 0.5	+2.7	A \rightarrow B
Leave-One-Out	9.2 \pm 1.2	+5.3	8 \rightarrow 1
Multi-Domain (Ex.)	37.2 \pm 3.8	+33	Joint
Single-Domain (Ex.)	54.6 \pm 5.5	+51	New probs
Plan-Variant	51.2 \pm 16.6	+47	New plans
Single-Domain (In.)	99.7 \pm 0.1	+96	Same probs

frozen embeddings capture essentially none of this structural commonality. Pre-trained embeddings support generalization only when training provides exposure to the target domain; they cannot transfer successfully to novel domain structures. We attribute this transfer failure partly to the domain-specificity of learned action semantics. While the action disambiguation loss substantially improves within-domain generalization (Appendix G.2), it does so by learning fine-grained distinctions among a domain’s actions, e.g., that `pick-up` (A) clears Block A while `stack` (A, B) does not. These learned distinctions are inherently tied to the source domain’s action space and provide limited benefit when the target domain uses different actions.

The gap structure reveals the bottleneck in latent planning. The $8 \times$ jump from Cross-Domain (6.6%) to Single-Domain Extrapolation (54.6%) far exceeds the $1.8 \times$ gain from Extrapolation to Interpolation (99.7%). Acquiring domain-specific transition knowledge accounts for most of the difficulty; once a model has seen a domain’s dynamics, it extrapolates reasonably to new problems within that domain. Learning from one domain, however, provides limited benefit for another. Training on all domains jointly offers a partial solution, as a unified model achieves 37.2%, underperforming single-domain specialists by 17 pp but retaining meaningful capability across all nine domains without catastrophic forgetting (Table 12). This gap represents the cost of generality, where a single model substitutes for nine specialists while preserving two-thirds of their average performance, confirms the model captures action-specific transformation patterns across domains.

5. Conclusion

This research introduces EMBEDPLAN, a framework for learning transition dynamics in frozen LLM embedding space, systematically evaluated across 9 planning domains, 4 encoders, and 6 generalization protocols. Our study demonstrates that frozen embeddings can support transition learning within known problem manifolds but fail to gener-

alize beyond them. Our findings delineate a sharp capability boundary: near-perfect interpolation (99.7%), meaningful extrapolation (54.6%, 14 \times above chance), and near-zero cross-domain transfer (6.6%). These results establish when frozen embeddings suffice, within-domain applications with sufficient training coverage, and when they do not, zero-shot transfer to novel domains.

The gap structure reveals that acquiring domain-specific transition knowledge, not generalizing within domains, is the primary bottleneck. Once exposed to a domain’s dynamics, models extrapolate reasonably to new problems; learning from one domain, however, provides essentially no benefit for another. We attribute this to how embeddings cluster by problem instance rather than structural role, placing functionally equivalent states in distant regions when variable names differ. This geometric fragmentation persists across encoder scales, confirming the limitation is architectural rather than capacity-based.

Plan-level evaluation provides evidence against pure trajectory memorization: models generalize to alternative optimal plans for training problems, suggesting they capture transferable transition dynamics rather than simply replaying observed sequences. Moreover, multi-domain training retains meaningful capability across all domains without catastrophic forgetting, indicating that a unified latent space can encode multiple transition functions simultaneously into universal latent planner.

5.1. Limitations and Future Work

We evaluate classical domains with templated descriptions; free-form language may behave differently. The framework uses frozen embeddings only; fine-tuning might address the clustering failure. Our retrieval formulation assumes pre-enumerated candidate pools, limiting applicability to open-ended generation settings. Training uses in-batch negatives sampled across problems while Extrapolation evaluation uses within-problem distractors; aligning these distributions during training may improve generalization. We do not benchmark wall-clock latency against autoregressive LLM planners, nor compare against symbolic compilation or object-centric dynamics models—such comparisons require end-to-end planning benchmarks beyond our diagnostic scope. Our plan-level evaluation uses teacher forcing to isolate transition quality; closed-loop evaluation with error accumulation remains future work. While our action disambiguation objective improves within-domain generalization, it learns domain-specific semantics that do not transfer across domain boundaries.

Several future directions emerge. First, embedding clustering by problem instance rather than structural role motivates planning-aware fine-tuning that groups functionally equivalent states regardless of variable names. Second,

object-centric architectures that factor states into entities and relations may better capture compositional structure, for multi-object domains. Third, the action disambiguation loss improves within-domain generalization but learns domain-specific semantics; action abstraction mechanisms that recognize shared operation types across domains (e.g., mapping “pick-up” and “board” to an abstract “acquire” schema) could improve cross-domain transfer. Finally, beyond pre-enumerated settings, predicted embeddings could guide constrained decoders to generate candidate states dynamically during search at runtime. Finally, the quantified capability boundary serves as a calibration for compositional generalization, defining frozen-representation limits.

Impact Statement

This paper characterizes capability boundaries for learning transition dynamics in frozen language embedding space. By replacing token-by-token generation with embedding-space prediction and retrieval, such methods could reduce computational cost for planning within known domains where state spaces are enumerable. Our experiments evaluate next-state retrieval accuracy in classical planning benchmarks rather than end-to-end decision-making or wall-clock latency in deployed systems.

Our experiments are limited to classical planning domains rendered as templated natural language and evaluate next-state retrieval accuracy rather than end-to-end decision-making in real-world environments. Accordingly, we focus on the most direct and tractable impacts of this contribution, rather than the full space of downstream applications. The primary risks are indirect. First, overstating generalization could motivate use in higher-stakes settings despite our findings of substantial out-of-distribution degradation and near-zero cross-domain transfer. Second, embedding-based retrieval may amplify sensitivity to surface form, leading to brittle behavior under paraphrase, underspecification, or distribution shift. Third, while the method amortizes runtime cost via cached embeddings and inexpensive transition prediction, large-scale embedding extraction can still incur nontrivial computational overhead.

We do not introduce new data collection involving human subjects, nor do we target applications that directly affect individuals’ rights or access to resources. As mitigation, we explicitly characterize failure modes across increasingly challenging generalization protocols and recommend that any practical use treat learned transitions as components requiring domain-specific validation, monitoring, and guardrails. Future work should evaluate robustness to free-form language, incorporate uncertainty estimation and abstention mechanisms, and investigate representations that better align embedding geometry with structural planning constraints to reduce brittleness under distribution shift.

References

Asai, M. and Fukunaga, A. Classical planning in deep latent space: Bridging the subsymbolic-symbolic boundary. In *Proceedings of the aaai conference on artificial intelligence*, volume 32, 2018.

Assran, M., Duval, Q., Misra, I., Bojanowski, P., Vincent, P., Rabbat, M., LeCun, Y., and Ballas, N. Self-supervised learning from images with a joint-embedding predictive architecture. In *Proceedings of the IEEE/CVF Conference on Computer Vision and Pattern Recognition*, pp. 15619–15629, 2023.

Battaglia, P. W., Hamrick, J. B., Bapst, V., Sanchez-Gonzalez, A., Zambaldi, V., Malinowski, M., Tacchetti, A., Raposo, D., Santoro, A., Faulkner, R., et al. Relational inductive biases, deep learning, and graph networks. *arXiv preprint arXiv:1806.01261*, 2018.

Gao, T., Yao, X., and Chen, D. Simcse: Simple contrastive learning of sentence embeddings. In *Proceedings of the 2021 Conference on Empirical Methods in Natural Language Processing*, pp. 6894–6910, 2021.

Gieselmann, R. and Pokorny, F. T. Latent planning via expansive tree search. *Advances in Neural Information Processing Systems*, 35:16821–16835, 2022.

Guan, L., Valmeekam, K., Sreedharan, S., and Kambhampati, S. Leveraging pre-trained large language models to construct and utilize world models for model-based task planning. *Advances in Neural Information Processing Systems*, 36:79081–79094, 2023.

Ha, D. and Schmidhuber, J. Recurrent world models facilitate policy evolution. *Advances in neural information processing systems*, 31, 2018.

Ha, D., Dai, A. M., and Le, Q. V. Hypernetworks. In *International Conference on Learning Representations*, 2017. URL <https://openreview.net/forum?id=rkpACellx>.

Hafner, D., Lillicrap, T., Fischer, I., Villegas, R., Ha, D., Lee, H., and Davidson, J. Learning latent dynamics for planning from pixels. In *International conference on machine learning*, pp. 2555–2565. PMLR, 2019.

Hafner, D., Lillicrap, T., Ba, J., and Norouzi, M. Dream to control: Learning behaviors by latent imagination. In *International Conference on Learning Representations*, 2020.

Hao, S., Gu, Y., Ma, H., Hong, J., Wang, Z., Wang, D., and Hu, Z. Reasoning with language model is planning with world model. In *Proceedings of the 2023 Conference on Empirical Methods in Natural Language Processing*, pp. 8154–8173, 2023.

Humphreys, P., Guez, A., Tieleman, O., Sifre, L., Weber, T., and Lillicrap, T. Large-scale retrieval for reinforcement learning. *Advances in Neural Information Processing Systems*, 35:20092–20104, 2022.

Kambhampati, S., Valmeekam, K., Guan, L., Verma, M., Stechly, K., Bhambri, S., Saldyt, L. P., and Murthy, A. B. Position: Llms can't plan, but can help planning in llm-modulo frameworks. In *Forty-first International Conference on Machine Learning*, 2024.

Katz, M., Kokel, H., Srinivas, K., and Sohrabi Araghi, S. Thought of search: Planning with language models through the lens of efficiency. *Advances in Neural Information Processing Systems*, 37:138491–138568, 2024.

Khandelwal, U., Levy, O., Jurafsky, D., Zettlemoyer, L., and Lewis, M. Generalization through memorization: Nearest neighbor language models. In *International Conference on Learning Representations*, 2020.

Kim, N. and Linzen, T. Cogs: A compositional generalization challenge based on semantic interpretation. In *Empirical Methods in Natural Language Processing*, 2020.

Kokel, H., Katz, M., Srinivas, K., and Sohrabi, S. Acp-bench: Reasoning about action, change, and planning. In *Proceedings of the AAAI Conference on Artificial Intelligence*, volume 39, pp. 26559–26568, 2025a.

Kokel, H., Katz, M., Srinivas, K., and Sohrabi, S. Acp-bench: Reasoning about action, change, and planning. In *Proceedings of the AAAI Conference on Artificial Intelligence*, volume 39, pp. 26559–26568, 2025b.

Lake, B. and Baroni, M. Generalization without systematicity: On the compositional skills of sequence-to-sequence recurrent networks. In *International conference on machine learning*, pp. 2873–2882. PMLR, 2018.

Laskin, M., Srinivas, A., and Abbeel, P. Curl: Contrastive unsupervised representations for reinforcement learning. In *International conference on machine learning*, pp. 5639–5650. PMLR, 2020.

Liu, B., Jiang, Y., Zhang, X., Liu, Q., Zhang, S., Biswas, J., and Stone, P. Llm+ p: Empowering large language models with optimal planning proficiency. *arXiv preprint arXiv:2304.11477*, 2023.

McDermott, D., Ghallab, M., Howe, A., Knoblock, C., Ram, A., Veloso, M., Weld, D., and Wilkins, D. PDDL – The Planning Domain Definition Language – Version 1.2. Technical Report CVC TR-98-003/DCS TR-1165, Yale Center for Computational Vision and Control, 1998.

Micheli, V., Alonso, E., and Fleuret, F. Transformers are sample-efficient world models. In *International Conference on Learning Representations*, 2023.

Muennighoff, N., Tazi, N., Magne, L., and Reimers, N. Mteb: Massive text embedding benchmark. In *Proceedings of the 17th Conference of the European Chapter of the Association for Computational Linguistics*, pp. 2014–2037, 2023.

Oord, A. v. d., Li, Y., and Vinyals, O. Representation learning with contrastive predictive coding. *arXiv preprint arXiv:1807.03748*, 2018.

Oswald, J., Srinivas, K., Kokel, H., Lee, J., Katz, M., and Sohrabi, S. Large language models as planning domain generators. In *Proceedings of the Thirty-Fourth International Conference on Automated Planning and Scheduling (ICAPS 2024)*, pp. 423–431. AAAI Press, 2024.

Oved, A., Shlomov, S., Zelty, S., Mashkif, N., and Yaeli, A. Snap: semantic stories for next activity prediction. In *Proceedings of the AAAI Conference on Artificial Intelligence*, volume 39, pp. 28871–28877, 2025.

Perez, E., Strub, F., De Vries, H., Dumoulin, V., and Courville, A. Film: Visual reasoning with a general conditioning layer. In *Proceedings of the AAAI conference on artificial intelligence*, volume 32, 2018.

Radford, A., Kim, J. W., Hallacy, C., Ramesh, A., Goh, G., Agarwal, S., Sastry, G., Askell, A., Mishkin, P., Clark, J., et al. Learning transferable visual models from natural language supervision. In *International conference on machine learning*, pp. 8748–8763. PMLR, 2021.

Reimers, N. and Gurevych, I. Sentence-bert: Sentence embeddings using siamese bert-networks. In *Proceedings of the 2019 Conference on Empirical Methods in Natural Language Processing and the 9th International Joint Conference on Natural Language Processing (EMNLP-IJCNLP)*, pp. 3982–3992, 2019.

Schrittwieser, J., Antonoglou, I., Hubert, T., Simonyan, K., Sifre, L., Schmitt, S., Guez, A., Lockhart, E., Hassabis, D., Graepel, T., et al. Mastering atari, go, chess and shogi by planning with a learned model. *Nature*, 588(7839): 604–609, 2020.

Schwarzer, M., Anand, A., Goel, R., Hjelm, R. D., Courville, A., and Bachman, P. Data-efficient reinforcement learning with self-predictive representations. In *International Conference on Learning Representations*, 2021.

Shinn, N., Cassano, F., Gopinath, A., Narasimhan, K., and Yao, S. Reflexion: Language agents with verbal reinforcement learning. *Advances in Neural Information Processing Systems*, 36:8634–8652, 2023.

Tantakoun, M., Muise, C., and Zhu, X. LLMs as planning formalizers: A survey for leveraging large language models to construct automated planning models. In Che, W., Nabende, J., Shutova, E., and Pilehvar, M. T. (eds.), *Findings of the Association for Computational Linguistics: ACL 2025*, pp. 25167–25188, Vienna, Austria, July 2025. Association for Computational Linguistics. ISBN 979-8-89176-256-5. doi: 10.18653/v1/2025.findings-acl.1291. URL <https://aclanthology.org/2025.findings-acl.1291/>.

Wei, J., Wang, X., Schuurmans, D., Bosma, M., Xia, F., Chi, E., Le, Q. V., Zhou, D., et al. Chain-of-thought prompting elicits reasoning in large language models. *Advances in neural information processing systems*, 35:24824–24837, 2022.

Yao, S., Zhao, J., Yu, D., Du, N., Shafran, I., Narasimhan, K. R., and Cao, Y. React: Synergizing reasoning and acting in language models. In *The eleventh international conference on learning representations*, 2022.

Yao, S., Yu, D., Zhao, J., Shafran, I., Griffiths, T., Cao, Y., and Narasimhan, K. Tree of thoughts: Deliberate problem solving with large language models. *Advances in neural information processing systems*, 36:11809–11822, 2023.

Zuo, M., Velez, F. P., Li, X., Littman, M., and Bach, S. Planetarium: A rigorous benchmark for translating text to structured planning languages. In Chiruzzo, L., Ritter, A., and Wang, L. (eds.), *Proceedings of the 2025 Conference of the Nations of the Americas Chapter of the Association for Computational Linguistics: Human Language Technologies (Volume 1: Long Papers)*, pp. 11223–11240, Albuquerque, New Mexico, April 2025. Association for Computational Linguistics. ISBN 979-8-89176-189-6. doi: 10.18653/v1/2025.nacl-long.560. URL <https://aclanthology.org/2025.nacl-long.560/>.

A. Evaluation Protocols

These protocols form a diagnostic hierarchy for capability characterization. We deliberately isolate transition accuracy from search algorithms, candidate generation, and latency measurement to provide clean assessment of what frozen embeddings support. End-to-end planning evaluation, while important for deployed systems, would conflate these factors.

We evaluate EMBEDPLAN under six protocols that measure progressively more demanding generalization capabilities. Let $\mathcal{D} = \{d_1, \dots, d_9\}$ denote the set of 9 planning domains. For each domain $d \in \mathcal{D}$, let $\mathcal{P}_d = \{p_1^d, \dots, p_{n_d}^d\}$ denote the set of problem instances, where $n_d = |\mathcal{P}_d|$. Each problem $p \in \mathcal{P}_d$ yields a set of transitions $\mathcal{T}_p = \{(s_i, a_i, s'_i)\}_{i=1}^{m_p}$ extracted from optimal plan trajectories, where $m_p = |\mathcal{T}_p|$.

The complete transition set for domain d is $\mathcal{T}_d = \bigcup_{p \in \mathcal{P}_d} \mathcal{T}_p$, and the global transition set across all domains is $\mathcal{T} = \bigcup_{d \in \mathcal{D}} \mathcal{T}_d$.

A.1. Protocol 1: Interpolation Split

Definition. Transitions are randomly partitioned regardless of problem or domain membership:

$$\mathcal{T}_d = \mathcal{T}_d^{\text{train}} \cup \mathcal{T}_d^{\text{test}}, \quad \mathcal{T}_d^{\text{train}} \cap \mathcal{T}_d^{\text{test}} = \emptyset \quad (4)$$

$$|\mathcal{T}_d^{\text{train}}| = 0.8 \cdot |\mathcal{T}_d|, \quad |\mathcal{T}_d^{\text{test}}| = 0.2 \cdot |\mathcal{T}_d| \quad (5)$$

where each transition $(s, a, s') \in \mathcal{T}_d$ is assigned to train or test uniformly at random.

Key Property. For any problem p , transitions may appear in both splits:

$$\exists p \in \mathcal{P}_d : \mathcal{T}_p \cap \mathcal{T}_d^{\text{train}} \neq \emptyset \wedge \mathcal{T}_p \cap \mathcal{T}_d^{\text{test}} \neq \emptyset \quad (6)$$

Measures. *Interpolation* within known problem manifolds. Models can succeed by recognizing which problem instance a state belongs to and applying memorized problem-specific transition patterns.

A.2. Protocol 2: Plan-Variant Split

Definition. Evaluate full-plan execution on alternative optimal plans for problems seen during training. Let $\Pi_p = \{\pi_1, \pi_2, \dots, \pi_k\}$ denote the set of optimal plans for problem p , where each plan π_i is a sequence of actions leading from initial state to goal. Plans are partitioned:

$$\Pi_p = \Pi_p^{\text{train}} \cup \Pi_p^{\text{test}}, \quad \Pi_p^{\text{train}} \cap \Pi_p^{\text{test}} = \emptyset \quad (7)$$

$$\mathcal{T}_p^{\text{train}} = \bigcup_{\pi \in \Pi_p^{\text{train}}} \mathcal{T}_\pi, \quad \mathcal{T}_p^{\text{test}} = \bigcup_{\pi \in \Pi_p^{\text{test}}} \mathcal{T}_\pi \quad (8)$$

where \mathcal{T}_π denotes the transitions extracted from plan π . Optimal plans are obtained directly from the dataset. For problems admitting multiple optimal solutions, we partition plans such that train and test contain non-overlapping action sequences. Problems with unique optimal plans are excluded from this protocol.

Key Property. Train and test share the same underlying problem instances, but differ in the action sequences used to reach the goal:

$$\forall p \in \mathcal{P}_d : \mathcal{P}_p^{\text{train}} = \mathcal{P}_p^{\text{test}} = \mathcal{P}_d, \text{ but } \Pi_p^{\text{train}} \cap \Pi_p^{\text{test}} = \emptyset \quad (9)$$

Measures. *Generalization to unseen solution paths under fixed problem structure.* Models must learn transition dynamics that transfer across different valid action sequences within the same problem, rather than memorizing specific plan trajectories. This tests whether the model captures the underlying state-action mechanics or merely overfits to observed plans.

A.3. Protocol 3: Extrapolation Split

Definition. Problems are partitioned, and all transitions from each problem go exclusively to train or test:

$$\mathcal{P}_d = \mathcal{P}_d^{\text{train}} \cup \mathcal{P}_d^{\text{test}}, \quad \mathcal{P}_d^{\text{train}} \cap \mathcal{P}_d^{\text{test}} = \emptyset \quad (10)$$

$$\mathcal{T}_d^{\text{train}} = \bigcup_{p \in \mathcal{P}_d^{\text{train}}} \mathcal{T}_p, \quad \mathcal{T}_d^{\text{test}} = \bigcup_{p \in \mathcal{P}_d^{\text{test}}} \mathcal{T}_p \quad (11)$$

with $|\mathcal{P}_d^{\text{train}}| \approx 0.8 \cdot |\mathcal{P}_d|$.

Key Property. Train and test transitions come from disjoint problem sets:

$$\forall p \in \mathcal{P}_d^{\text{test}} : \mathcal{T}_p \cap \mathcal{T}_d^{\text{train}} = \emptyset \quad (12)$$

Measures. *Extrapolation* to new problem configurations within a known domain. Models must learn transferable domain dynamics (e.g., “pick-up removes a block from a surface”) rather than problem-specific patterns.

A.4. Protocol 4: Multi-Domain Learning (Unified Model)

Definition. Train a single model on all domains simultaneously, with Extrapolation splits within each domain:

$$\mathcal{T}^{\text{train}} = \bigcup_{d \in \mathcal{D}} \mathcal{T}_d^{\text{train}}, \quad \text{where } \mathcal{T}_d^{\text{train}} = \bigcup_{p \in \mathcal{P}_d^{\text{train}}} \mathcal{T}_p \quad (13)$$

$$\mathcal{T}^{\text{test}} = \bigcup_{d \in \mathcal{D}} \mathcal{T}_d^{\text{test}}, \quad \text{where } \mathcal{T}_d^{\text{test}} = \bigcup_{p \in \mathcal{P}_d^{\text{test}}} \mathcal{T}_p \quad (14)$$

A single transition network $T_{\theta}^{\text{multi}}$ is trained on $\mathcal{T}^{\text{train}}$ and evaluated per-domain:

$$\text{Multi-Domain}(d) = \text{Hit}@k(T_{\theta}^{\text{multi}}, \mathcal{T}_d^{\text{test}}) \quad (15)$$

Key Property. The model must represent 9 distinct transition functions in a shared parameter space:

$$T_{\theta}^{\text{multi}} : \mathbb{R}^{128} \times \mathbb{R}^{128} \rightarrow \mathbb{R}^{128}, \quad \forall d \in \mathcal{D} \quad (16)$$

Measures. *Capacity sharing without catastrophic forgetting.* Tests whether a unified 128-dimensional latent space can encode transition dynamics for multiple domains simultaneously.

A.5. Protocol 5: Cross-Domain Transfer (Zero-Shot)

Definition. Train on one source domain, evaluate on a different target domain:

$$\mathcal{T}^{\text{train}} = \mathcal{T}_{d_{\text{src}}}, \quad d_{\text{src}} \in \mathcal{D} \quad (17)$$

$$\mathcal{T}^{\text{test}} = \mathcal{T}_{d_{\text{tgt}}}, \quad d_{\text{tgt}} \in \mathcal{D} \setminus \{d_{\text{src}}\} \quad (18)$$

For comprehensive evaluation, we compute performance for all source-target pairs:

$$\begin{aligned} \text{Cross-Domain}(d_{\text{tgt}}) &= \frac{1}{|\mathcal{D}| - 1} \sum_{d_{\text{src}} \neq d_{\text{tgt}}} \\ &\quad \text{Hit}@k(T_{\theta}^{d_{\text{src}}}, \mathcal{T}_{d_{\text{tgt}}}). \end{aligned} \quad (19)$$

where $T_{\theta}^{d_{\text{src}}}$ denotes the transition network trained on domain d_{src} .

Key Property. No overlap in domains, problems, or transitions between train and test:

$$\mathcal{T}^{\text{train}} \cap \mathcal{T}^{\text{test}} = \emptyset, \quad \mathcal{P}_{d_{\text{src}}} \cap \mathcal{P}_{d_{\text{tgt}}} = \emptyset \quad (20)$$

Measures. *Zero-shot domain transfer.* Models must learn transition dynamics that generalize across fundamentally different planning structures (e.g., from block manipulation to logistics).

A.6. Protocol 6: Leave-One-Out Generalization (LOO)

Definition. Train on $|\mathcal{D}| - 1$ domains, evaluate on the held-out domain:

$$\mathcal{T}^{\text{train}} = \bigcup_{d \in \mathcal{D} \setminus \{d_{\text{held}}\}} \mathcal{T}_d \quad (21)$$

$$\mathcal{T}^{\text{test}} = \mathcal{T}_{d_{\text{held}}} \quad (22)$$

For comprehensive evaluation, we iterate over all held-out domains:

$$\text{LOO}(d_{\text{held}}) = \text{Hit}@k(T_{\theta}^{\mathcal{D} \setminus \{d_{\text{held}}\}}, \mathcal{T}_{d_{\text{held}}}) \quad (23)$$

Key Property. Unlike Cross-Domain (single source), LOO provides maximum training diversity:

$$|\mathcal{T}^{\text{train}}| = \sum_{d \neq d_{\text{held}}} |\mathcal{T}_d| \gg |\mathcal{T}_{d_{\text{src}}}| \quad (\text{Cross-Domain}) \quad (24)$$

Measures. *Transfer from diverse training to unseen domain.* Tests whether exposure to 8 diverse domains enables generalization to an entirely novel 9th domain.

A.7. Protocol Hierarchy

The six protocols form a hierarchy of increasing generalization difficulty:

Protocol	Measures	Shared Domain	Shared Problems	Shared Plans	Difficulty
Interpolation	Interpolation	✓	✓	✓	Lowest
Plan-Variant	Plan generalization	✓	✓	✗	Low
Extrapolation	Extrapolation	✓	✗	✗	Medium
Multi-Domain	Capacity sharing	✓	✗	✗	Medium
Cross-Domain	Zero-shot transfer	✗	✗	✗	High
Leave-One-Out	Diverse transfer	✗	✗	✗	Highest

Table 5. Evaluation protocol hierarchy by generalization difficulty.

Design Rationale. This hierarchy isolates where frozen embeddings succeed versus fail:

- **Interpolation → Plan-Variant:** Quantifies overfitting to specific action sequences
- **Plan-Variant → Extrapolation:** Quantifies the interpolation-extrapolation gap
- **Extrapolation → Multi-Domain:** Tests capacity sharing
- **Multi-Domain → Cross-Domain/LOO:** Tests zero-shot transfer

B. Experimental Setup

B.1. Architecture

Figure 4 provides a complete illustration of the EMBEDPLAN architecture.

B.1.1. FROZEN ENCODERS

States and actions are encoded using frozen pretrained language models. We experiment with four encoders spanning different architectures and scales:

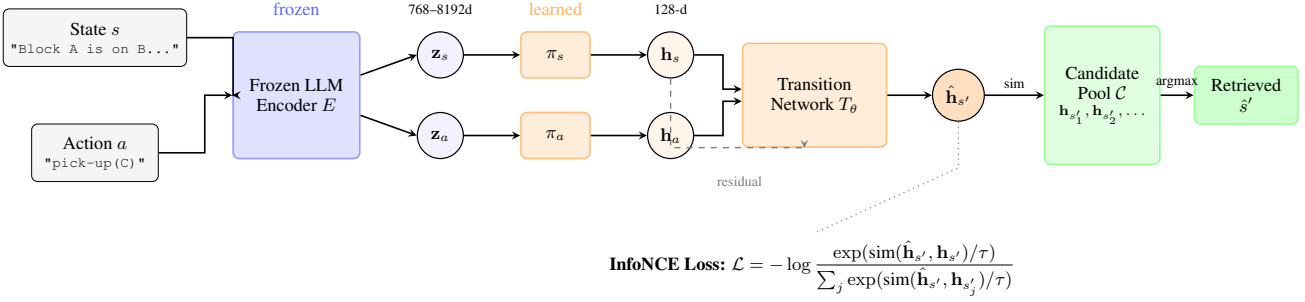


Figure 4. Complete EMBEDPLAN Architecture. State and action descriptions are encoded by a frozen LLM encoder E into high-dimensional embeddings $\mathbf{z}_s, \mathbf{z}_a$. Learned projection heads π_s, π_a reduce dimensionality to a shared 128-d space. The transition network T_θ (with residual connection from \mathbf{h}_s) predicts the next-state embedding $\hat{\mathbf{h}}_{s'}$, trained via InfoNCE to maximize similarity to the ground-truth embedding. At inference, the model retrieves the most similar state from a candidate pool.

MPNet (all-mpnet-base-v2). A 110-million parameter sentence transformer (Reimers & Gurevych, 2019) trained on over 1 billion sentence pairs. This model produces 768-dimensional embeddings optimized for semantic similarity tasks. We use the sentence-transformers library with default mean pooling.

BGE-M3 (BAAI/bge-m3). A state-of-the-art multilingual embedding model (568M parameters) designed for multi-granularity retrieval. We utilize the dense retrieval component, which extracts 1024-dimensional embeddings from the [CLS] token of the final layer.

Qwen2.5-7B-Instruct. A 7-billion parameter instruction-tuned autoregressive model. We extract sentence embeddings by applying mean pooling over the final layer’s hidden states, producing 3584-dimensional embeddings.

Llama-3.3-70B-70B-Instruct. A 70-billion parameter autoregressive language model. Since decoder-only models do not have a natural sentence embedding, we apply mean pooling over the final layer’s hidden states across all input tokens:

$$\mathbf{z} = \frac{1}{T} \sum_{t=1}^T \mathbf{h}_t^{(L)} \quad (25)$$

where $\mathbf{h}_t^{(L)} \in \mathbb{R}^{8192}$ is the hidden state at position t in the final layer L , and T is the sequence length. Mean pooling over decoder-only hidden states is a common approximation when dedicated sentence embeddings are unavailable (Muenninghoff et al., 2023). While task-specific pooling strategies (e.g., last-token with EOS prompting) may yield different representations, we adopt mean pooling for consistency across autoregressive architectures and leave pooling sensitivity analysis to future work.

Rationale for Freezing. We freeze encoders for two reasons. First, it isolates our research question: we test whether *existing* pretrained representations support transition learning, without confounding this with task-specific fine-tuning that might introduce planning structure. Second, it enables efficient experimentation: embeddings are computed once and cached, reducing each training run from hours of LLM inference to minutes of lightweight optimization.

Pooling Strategy Rationale. We adopt mean pooling uniformly across decoder-only models for consistency, acknowledging that this is one of several reasonable choices. Instruction-tuned sentence encoders or last-token pooling with explicit EOS prompting may yield embeddings better suited for semantic similarity; our results thus represent a lower bound on what optimized embedding extraction could achieve. We prioritize architectural consistency across encoders over per-encoder optimization.

B.1.2. PROJECTION HEADS

High-dimensional encoder outputs present computational and statistical challenges. We introduce learnable projection heads that map to a lower-dimensional space where transition learning occurs.

Each projection head is a multi-layer perceptron:

$$\pi(\mathbf{z}) = W_L \sigma(\text{LN}(W_{L-1} \sigma(\text{LN}(W_1 \mathbf{z})))) \quad (26)$$

where $\sigma(\cdot)$ denotes GELU activation and $\text{LN}(\cdot)$ denotes layer normalization. We use separate projection heads for states (π_s) and actions (π_a), allowing each to learn modality-specific transformations.

Default Configuration.

- Input dimension: encoder-dependent (768 for MPNet, 1024 for BGE-M3, 3584 for Qwen, 8192 for Llama)
- Output dimension: 128
- Hidden layers: 4
- Activation: GELU
- Normalization: LayerNorm after each hidden layer

B.1.3. TRANSITION NETWORK

We investigate two architectures embodying different hypotheses about how actions transform states.

Residual MLP (Primary). Our primary architecture processes the concatenated state-action representation through a feedforward network with a residual connection:

$$\hat{\mathbf{h}}_{s'} = \text{LN}\left(f_\theta([\mathbf{h}_s; \mathbf{h}_a]) + W_{\text{res}} \mathbf{h}_s\right) \quad (27)$$

The feedforward network f_θ has architecture:

$$f_\theta(\mathbf{x}) = W_3 \sigma(W_2 \sigma(W_1 \mathbf{x})) \quad (28)$$

with dimensions $W_1 : \mathbb{R}^{256} \rightarrow \mathbb{R}^{128}$, $W_2 : \mathbb{R}^{128} \rightarrow \mathbb{R}^{128}$, $W_3 : \mathbb{R}^{128} \rightarrow \mathbb{R}^{128}$.

The residual term $W_{\text{res}} \mathbf{h}_s$ encodes an inductive bias: actions produce *incremental modifications* to states rather than wholesale replacements. Most predicates remain unchanged after a single action; only a few flip.

HyperNetwork (Alternative). An alternative hypothesis is that different actions require fundamentally different transformations. We implement this via a hypernetwork (Ha et al., 2017) that generates action-conditioned modulation parameters:

$$g_\phi(\mathbf{h}_a) = W_g^{(2)} \sigma(W_g^{(1)} \mathbf{h}_a) \in \mathbb{R}^{2L \cdot d_{\text{adapt}}} \quad (29)$$

This output is split into L pairs of scale and shift vectors $(\mathbf{A}_i, \mathbf{b}_i)$ for FiLM-style conditioning (Perez et al., 2018).

B.2. Training Details

B.2.1. TRAINING OBJECTIVE

We train with InfoNCE (Oord et al., 2018), a contrastive loss that operates on batches of transitions:

$$\mathcal{L} = -\frac{1}{B} \sum_{i=1}^B \log \frac{\exp(\text{sim}(\hat{\mathbf{h}}_{s'_i}, \mathbf{h}_{s'_i})/\tau)}{\sum_{j=1}^B \exp(\text{sim}(\hat{\mathbf{h}}_{s'_i}, \mathbf{h}_{s'_j})/\tau)} \quad (30)$$

where $\text{sim}(\mathbf{u}, \mathbf{v}) = \mathbf{u}^\top \mathbf{v} / (\|\mathbf{u}\| \|\mathbf{v}\|)$ is cosine similarity, $\tau = 0.07$ is temperature, and $B = 128$ is batch size.

In-Batch Negatives. The denominator treats all B states in the batch as candidates, with the $B-1$ non-matching states serving as negatives. This provides 127 negatives per positive without additional computation.

Why Contrastive? Contrastive learning offers advantages over regression losses: (1) scale invariance via cosine similarity, (2) direct optimization of the retrieval objective, and (3) natural hard negative mining from same-domain states in the batch.

B.2.2. LOSS FORMULATIONS

The state prediction loss uses InfoNCE over batch elements:

$$\mathcal{L}_{\text{state}} = -\frac{1}{B} \sum_{i=1}^B \log \frac{\exp(\text{sim}(\hat{\mathbf{h}}_{s'_i}, \mathbf{h}_{s'_i})/\tau)}{\sum_{j=1}^B \exp(\text{sim}(\hat{\mathbf{h}}_{s'_i}, \mathbf{h}_{s'_j})/\tau)} \quad (31)$$

where $\text{sim}(\mathbf{u}, \mathbf{v}) = \mathbf{u}^\top \mathbf{v} / (\|\mathbf{u}\| \|\mathbf{v}\|)$ is cosine similarity and $\tau = 0.07$ is temperature.

The action disambiguation loss contrasts predictions from different actions applied to the same state:

$$\mathcal{L}_{\text{action}} = -\frac{1}{B} \sum_{i=1}^B \log \frac{\exp(z_{i,i}/\tau)}{\sum_{k=1}^K \exp(z_{i,k}/\tau)}, \quad (32)$$

$$z_{i,k} := \text{sim}(\hat{\mathbf{h}}_{s'_i}^{(a_k)}, \mathbf{h}_{s'_i})$$

where $\{\hat{\mathbf{h}}_{s'_i}^{(a_k)}\}_{k=1}^K$ are predictions from applying each of K ground actions to state s .

B.2.3. HYPERPARAMETER CONFIGURATION

Table 6 lists the hyperparameter search space and final configuration.

Hyperparameter	Values Explored
<i>Architecture</i>	
Model Type	MLP , HyperNetwork
Hidden Size	128 , 256
Number of Layers	2 , 4
Dropout	0.0 , 0.5
Layer Normalization	Yes
<i>Loss Function</i>	
Action Loss Weight (λ)	0, 0.5, 1, 1.5, 2 , 4
<i>Projection Head</i>	
Use Projection	Yes , No
Projection Dimension	128
Projection Layers	2 , 4
<i>Optimization</i>	
Learning Rate	2e-3, 1e-3, 4e-5
Batch Size	64, 128
InfoNCE Temperature (τ)	0.07
Weight Decay	1e-2
<i>Training</i>	
Max Epochs	400
Warmup Epochs	10
Early Stopping Patience	100

Table 6. Hyperparameter search space. Bold values indicate final configuration.

B.3. Evaluation Protocol

Hit@ k Computation. For each test transition (s, a, s') :

1. Compute predicted embedding: $\hat{\mathbf{h}}_{s'} = T_\theta(\pi_s(\mathbf{z}_s), \pi_a(\mathbf{z}_a))$

2. Compute similarity to all candidates: $\text{sim}_j = \text{sim}(\hat{\mathbf{h}}_{s'}, \mathbf{h}_{s'_j})$ for $s'_j \in \mathcal{C}$
3. Rank candidates by similarity (descending)
4. Record hit if correct s' appears in top- k

The candidate pool \mathcal{C} contains 128 states: the ground-truth next state plus 127 distractors sampled according to the evaluation protocol (uniformly from the domain for Interpolation; from the same problem instance for Extrapolation).

Tie-Breaking. When multiple candidates have identical similarity scores, we take one of them randomly.

Action Disambiguation. Given a state s and ground-truth next state s' , we apply all possible actions of the domain and check which prediction best matches s' :

$$\hat{a} = \arg \max_{a \in \mathcal{A}} \text{sim}(T_\theta(\mathbf{h}_s, \mathbf{h}_a), \mathbf{h}_{s'}) \quad (33)$$

Accuracy measures how often \hat{a} matches the true action.

B.4. Compute Resources

All experiments were conducted on the following infrastructure:

- **GPU:** NVIDIA A100 80GB
- **CPU:** AMD EPYC 7763 64-Core Processor
- **Memory:** 512GB RAM
- **Framework:** PyTorch 2.1, CUDA 12.1

Training Time.

- Embedding extraction (per domain, Llama-3.3-70B): ~ 2 hours
- Embedding extraction (per domain, MPNet): ~ 5 minutes
- Transition network training (per domain): ~ 15 minutes
- Full experimental suite (all encoders, all protocols): ~ 72 hours

Carbon Footprint. Estimated total compute: ~ 200 GPU-hours on A100. Using a carbon intensity of 0.4 kg CO₂/kWh and A100 TDP of 400W, estimated emissions: ~ 32 kg CO₂.

C. Dataset

C.1. Dataset Statistics

We use 9 classical PDDL domains from planning benchmarks (Kokel et al., 2025a). Table 7 summarizes the dataset. Note: our transition datasets are derived from ACPBench domains but involve additional processing not included in the publicly released dataset. We will release our processed data upon acceptance.

C.2. State Representation

States are rendered as natural language descriptions containing the current predicate values. Example from Blocksworld:

“Block A is on the table. Block B is on Block A. Block C is clear. The robotic arm is empty.”

Actions are parameterized strings (e.g., `pick-up(BlockC)`, `stack(BlockA, BlockB)`).

Domain	Problems	States	Transitions	Actions
Blocksworld	5	43,551	43,065	4
Depot	7	5,795	13,256	5
Ferry	10	46,205	225,300	3
Floortile	6	33,608	166,565	6
Goldminer	7	12,237	52,023	7
Grid	5	8,671	664,346	5
Logistics	7	13,373	46,866	6
Rovers	10	46,783	509,457	9
Satellite	10	49,204	1,248,696	4
Total	67	259,427	2,969,574	—

Table 7. Dataset statistics by domain.

Blocksworld

State s : Block block_2 is on the table, Block block_3 is located on the table, No blocks are placed on top of block_1, The block block_2 is currently situated under the block block_1, The robotic arm is not holding anything, and Block block_3 is clear.

Action a : (pick-up block_3)

Result s' : Block block_1 is clear, Block block_2 is located on the table, The robotic arm is holding block_3, and The block block_2 is currently situated under the block block_1.

C.3. Domain Descriptions

Blocksworld. A robotic arm must rearrange colored blocks into a specified goal configuration. Only clear blocks (with nothing on top) can be moved. This domain is renowned for simple rules yet rich combinatorial complexity.

Depot. Combines logistics and block stacking. Crates must be moved between depots using trucks for transportation and hoists for stacking/unstacking.

Ferry. A ferry boat transports cars between locations. The ferry can carry only one car at a time, requiring optimization of loading/unloading sequences.

Floortile. Robots paint floor tiles in a grid according to a target pattern. Robots must navigate while managing limited paint supplies and adjacency constraints.

Goldminer. An agent navigates a grid to collect gold pieces and deliver them to goal locations while managing inventory limits.

Grid. An agent moves on a 2D grid to reach target locations, potentially with obstacles restricting movement.

Logistics. Packages must be delivered within and across cities. Trucks handle intra-city transport; airplanes handle inter-city deliveries.

Rovers. Planetary exploration with multiple rovers collecting samples, taking images, and transmitting data. Rovers have specialized equipment and must communicate with a base station.

Satellite. Multiple satellites with various instruments must photograph ground targets while managing power, storage, and instrument calibration.

Ferry

State s : Car c0 is at location l0, Car c2 is at location l1, The ferry is at l0, and Car c1 is on the ferry.

Action a : (debark c1 10)

Result s' : Car c0 is at location l0, Car c1 is at location l0, The ferry is at l0, The ferry is empty, and Car c2 is at location l1.

Logistics

State s : p3 is in t1, a0 is at l0-0, t1 is at l1-0, p0 is at l1-0, p1 is in t1, t0 is at l0-0, and p2 is in a0.

Action a : (fly-airplane a0 l0-0 l1-0)

Result s' : t1 is at l1-0, p0 is at l1-0, p1 is in t1, p3 is in t1, t0 is at l0-0, a0 is at l1-0, and p2 is in a0.

C.4. Transition Examples

D. Extended Results

D.1. Per-Domain Results

Table 8 provides complete per-domain breakdown across encoders and evaluation protocols.

Domain	Qwen2.5-7B		Llama-3.3-70B	
	Int.	Ext.	Int.	Ext.
Blocksworld	100.0	41.6±15	100.0	49.1±10
Depot	98.2	24.8±9	98.8	25.9±6
Ferry	99.9	36.7±1	100.0	40.6±3
Floortile	99.4	55.2±19	99.6	68.8±16
Goldminer	99.9	74.4±10	100.0	76.2±5
Grid	98.6	62.7±9	99.8	74.9±1
Logistics	99.6	44.7±20	99.9	53.7±10
Rovers	99.7	49.2±3	99.0	54.4±3
Satellite	99.9	40.0±1	99.9	47.5±6
Mean	99.5	47.7±14	99.7	54.6±17

Table 8. Per-domain Hit@5 (%) for Interpolation and Extrapolation splits.

D.2. Full Performance Metrics

Table 9 reports Hit@1/5/10 and action accuracy for Problem-Grouped evaluation.

The gap between Hit@5 (54.6%) and Acc@5 (16.2%) reveals that models predict correct next states without fully capturing causal action structure.

D.3. Cross-Domain Transfer Matrix

Table 10 shows the complete 9×9 transfer matrix.

The only notable transfer is Ferry→Logistics (22.3%), which we attribute to shared transportation semantics in state descriptions.

D.4. Leave-One-Out Results

Despite training on 8 diverse domains, LOO performance (9.2%) barely exceeds the untrained baseline (3.9%).

Rovers

State s : Store(s) store0 is empty, Channel general is free, Image objective1 was communicated in mode colour, Rover rover0 has image objective1 in mode colour, Rover rover1 has soil analyzed in waypoint waypoint0, Rover rover1 is available, Rover rover1 is at waypoint0, Rocks can be sampled at the following location(s): waypoint0, Store(s) store1 is empty, Rover rover0 is available, and Rover rover0 is at waypoint2.

Action a : (communicate_soil_data rover1 general waypoint0 waypoint0 waypoint1)

Result s' : Store(s) store0 is empty, Channel general is free, Rover rover0 has image objective1 in mode colour, Image objective1 was communicated in mode colour, Rover rover1 has soil analyzed in waypoint waypoint0, Rover rover1 is available, Rover rover1 is at waypoint0, Rocks can be sampled at the following location(s): waypoint0, Soil data was communicated from waypoint waypoint0, Store(s) store1 is empty, Rover rover0 is available, and Rover rover0 is at waypoint2.

Domain	State Prediction			Action Accuracy		
	Hit@1	Hit@5	Hit@10	Acc@1	Acc@5	Acc@10
Blocksworld	17.6 \pm 9	49.1 \pm 17	64.6 \pm 13	0.7 \pm 0.2	7.9 \pm 2	24.0 \pm 4
Depot	4.7 \pm 2	25.9 \pm 11	41.2 \pm 14	0.7 \pm 0.4	7.8 \pm 3	21.8 \pm 4
Ferry	12.0 \pm 3	40.6 \pm 6	58.1 \pm 7	1.1 \pm 0.7	10.3 \pm 2	23.7 \pm 4
Floortile	37.6 \pm 22	68.8 \pm 27	78.9 \pm 22	3.2 \pm 1	28.3 \pm 15	52.3 \pm 25
Goldminer	35.8 \pm 11	76.2 \pm 9	88.0 \pm 3	3.0 \pm 0.4	16.5 \pm 2	45.7 \pm 6
Grid	25.7 \pm 2	74.9 \pm 2	88.0 \pm 2	8.0 \pm 4	50.0 \pm 8	73.9 \pm 10
Logistics	16.5 \pm 6	53.7 \pm 17	70.8 \pm 17	0.6 \pm 0.5	8.4 \pm 3	25.3 \pm 3
Rovers	16.9 \pm 2	54.4 \pm 5	72.2 \pm 4	0.9 \pm 0.1	7.1 \pm 0.4	16.5 \pm 3
Satellite	14.4 \pm 4	47.5 \pm 10	66.9 \pm 10	0.9 \pm 0.3	9.1 \pm 2	23.5 \pm 7
Mean	20.1 \pm 11	54.6 \pm 17	69.9 \pm 14	2.1 \pm 2	16.2 \pm 14	34.1 \pm 19

Table 9. Full metrics (Llama-3.3-70B, Problem-Grouped). Action accuracy measures whether the correct action is identified given (s, s') .

D.5. Multi-Domain Results

D.6. Untrained Baseline

To establish a performance floor, we evaluated the transition function with randomly initialized weights.

The untrained baseline (3.9% Hit@5) confirms the retrieval task’s inherent difficulty and that learned performance results from actual dynamics learning.

D.7. Plan-Level Evaluation Across Encoders

We extend our evaluation to the trajectory level to assess whether high transition accuracy translates to reliable multi-step planning. We compare two splitting strategies:

- **Interpolation:** Test plans come from problem instances seen during training (though the specific plans are held out).
- **Extrapolation:** Test plans come from entirely new problem instances never seen during training.

We report two metrics:

- **Mean Trajectory Hit@5:** Average Hit@5 across all steps in a trajectory.
- **Exact Trajectory Hit@5:** Percentage of trajectories where *every* step is correctly retrieved (100% reliability).

Tables 14–16 present results across three encoders. We observe a consistent **Trajectory Generalization Gap** across all models. Under Interpolation, models achieve moderate reliability, though Exact Match rates remain low due to error accumulation. Under Extrapolation, performance collapses dramatically—for Blocksworld, the Exact Trajectory rate falls to 0.0% across all encoders.

	Block	Depot	Ferry	Floor	Gold	Grid	Logis	Rover	Satel	Mean
Blocksworld	–	5.7	5.5	6.7	6.1	6.5	9.2	5.1	5.3	6.3
Depot	4.3	–	5.3	4.8	5.0	4.9	6.0	7.5	5.4	5.4
Ferry	5.3	8.7	–	9.3	5.2	9.0	22.3	6.6	5.6	9.0
Floortile	5.0	7.3	7.0	–	6.1	6.5	7.5	10.0	7.9	7.2
Goldminer	4.2	5.4	5.7	5.0	–	7.5	5.4	5.9	4.9	5.5
Grid	5.4	6.6	8.6	9.0	10.4	–	14.3	5.9	5.4	8.2
Logistics	4.3	5.5	7.7	4.9	7.0	6.3	–	5.1	4.5	5.7
Rovers	4.3	5.7	5.0	8.4	4.6	5.9	4.8	–	8.2	5.9
Satellite	4.5	7.5	6.3	7.8	6.4	5.2	10.1	5.9	–	6.7
Mean	4.7	6.5	6.4	7.0	6.4	6.5	9.9	6.5	5.9	6.6

Table 10. Cross-domain transfer (Llama-3.3-70B). Hit@5 (%) training on row, testing on column. Baseline: 3.9%.

Held-Out	Hit@1	Hit@5	Hit@10
Logistics	3.3±0.4	15.8±2.2	27.6±3.3
Grid	2.3±0.2	12.3±0.8	22.9±1.4
Rovers	2.6±0.3	12.6±1.1	22.6±1.6
Ferry	1.8±0.1	9.0±0.5	17.2±0.8
Satellite	1.6±0.1	8.4±0.8	16.1±1.5
Floortile	1.7±0.3	7.9±1.1	14.9±2.0
Goldminer	1.3±0.0	6.4±0.2	12.5±0.3
Depot	1.1±0.1	5.6±0.5	10.9±0.9
Blocksworld	1.0±0.0	5.2±0.1	10.3±0.3
Mean	1.9±0.7	9.2±3.5	17.2±5.8

Table 11. Leave-One-Out (Llama-3.3-70B). Train on 8 domains, test on held-out.

This confirms that the transition model’s planning capability is largely confined to memorized problem manifolds; when forced to extrapolate to new problems, the probability of executing a valid multi-step plan drops to near zero.

Key Observations.

- **Interpolation performance scales with encoder size:** Llama-3.3-70B and BGE-M3 achieve similar Mean Hit@5 (~51–53%), while MPNet lags significantly (24.3%).
- **Extrapolation collapse is universal:** All encoders show dramatic degradation under Extrapolation, with Exact Hit@5 dropping below 4% on average.
- **Domain-specific patterns persist:** Goldminer and Grid show relatively better Extrapolation performance across all encoders, while Blocksworld and Satellite consistently fail.
- **MPNet struggles even with Interpolation:** Rovers and Satellite show near-zero performance even under Interpolation, suggesting these domains require higher-capacity embeddings.

E. Statistical Analysis

E.1. Main Generalization Gap

See Table 17.

E.2. Effect Sizes for Key Comparisons

See Table 18.

E.3. Per-Domain Statistical Tests

See Table 19.

Domain	Hit@5	Domain	Hit@5
Floortile	52.0 \pm 10	Blocksworld	36.9 \pm 13
Rovers	51.9 \pm 5	Satellite	34.3 \pm 7
Goldminer	46.0 \pm 8	Grid	32.6 \pm 1
Ferry	37.7 \pm 14	Logistics	24.8 \pm 10
		Depot	18.9 \pm 12

Mean: 37.2 \pm 10.7 (vs. 54.6 single-domain)

Table 12. Multi-domain unified model (Llama-3.3-70B, Problem-Grouped).

Domain	Hit@1	Hit@5	Hit@10
Blocksworld	0.8 \pm 0.1	4.0 \pm 0.2	8.0 \pm 0.4
Depot	0.9 \pm 0.2	3.9 \pm 0.0	8.0 \pm 0.4
Ferry	0.7 \pm 0.1	4.3 \pm 0.6	8.4 \pm 0.9
Floortile	0.8 \pm 0.0	4.0 \pm 0.1	8.0 \pm 0.1
Goldminer	1.0 \pm 0.4	4.8 \pm 1.4	8.9 \pm 2.0
Grid	0.9 \pm 0.1	4.4 \pm 0.3	8.0 \pm 0.2
Logistics	0.9 \pm 0.1	4.1 \pm 0.2	8.6 \pm 0.6
Rovers	0.7 \pm 0.0	4.1 \pm 0.2	8.4 \pm 0.1
Satellite	0.7 \pm 0.0	3.9 \pm 0.1	7.8 \pm 0.1
Mean	0.8 \pm 0.1	3.9 \pm 0.3	8.2 \pm 0.4

Table 13. Untrained baseline (random weights, Llama-3.3-70B).

All comparisons remain significant after Bonferroni correction ($\alpha = 0.05/9 = 0.0056$) except Floortile and Goldminer, which are significant at uncorrected $\alpha = 0.05$.

F. Embedding Analysis

F.1. PCA Visualization

Figure 5 compares embedding geometry across model scales.

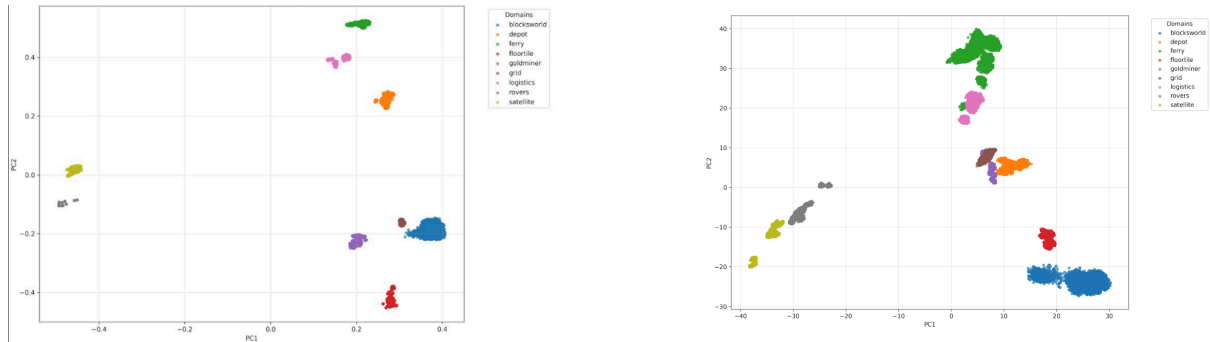


Figure 5. Embedding Space Fragmentation Across Scales. PCA visualization of state embeddings colored by problem instance. (A) MPNet embeddings show tight, isolated clusters for each problem. (B) Llama-3.3-70B-70B embeddings, despite being 700 \times larger, exhibit the same fragmentation. This confirms that pre-trained embeddings primarily cluster by problem-specific lexical features rather than abstract planning roles, regardless of model scale.

Both MPNet and Llama show isolated clusters corresponding to specific problem instances. While Llama shows slightly more spread within clusters, the critical structural limitation remains: manifolds for different problems are disjoint. Scaling up model parameters does not automatically induce abstract, problem-invariant representations.

Domain	Interpolation		Extrapolation	
	Mean Hit@5	Exact Hit@5	Mean Hit@5	Exact Hit@5
Blocksworld	38.7 ± 0.8	1.6 ± 0.2	3.7 ± 1.3	0.0 ± 0.0
Depot	30.1 ± 2.6	11.2 ± 1.5	2.4 ± 1.7	1.0 ± 1.0
Ferry	71.1 ± 1.1	39.1 ± 1.6	2.0 ± 0.7	0.5 ± 0.2
Floortile	74.1 ± 2.7	33.6 ± 3.3	11.6 ± 4.4	2.8 ± 1.2
Goldminer	55.4 ± 2.2	23.8 ± 1.6	18.5 ± 6.2	5.5 ± 1.8
Grid	55.0 ± 2.4	37.4 ± 2.2	16.6 ± 3.7	8.2 ± 2.1
Logistics	52.8 ± 0.6	14.1 ± 2.0	22.7 ± 8.6	9.6 ± 4.4
Rovers	26.5 ± 0.8	10.0 ± 0.7	12.2 ± 3.5	1.9 ± 0.8
Satellite	56.8 ± 1.2	32.2 ± 1.0	1.2 ± 0.4	0.5 ± 0.1
Mean	51.2 ± 16.6	22.6 ± 13.7	10.1 ± 8.0	3.3 ± 3.5

Table 14. Plan-Level Evaluation (Llama-3.3-70B-70B). Trajectory metrics across Interpolation and Extrapolation.

Domain	Interpolation		Extrapolation	
	Mean Hit@5	Exact Hit@5	Mean Hit@5	Exact Hit@5
Blocksworld	23.7 ± 1.5	0.2 ± 0.1	1.0 ± 0.4	0.0 ± 0.0
Depot	45.5 ± 1.0	20.9 ± 0.1	3.0 ± 1.4	1.1 ± 0.6
Ferry	63.3 ± 1.4	27.8 ± 2.1	5.4 ± 4.5	2.4 ± 2.2
Floortile	49.2 ± 1.0	13.1 ± 1.1	3.4 ± 1.2	0.6 ± 0.3
Goldminer	67.9 ± 2.6	35.0 ± 3.2	23.1 ± 3.2	9.4 ± 1.7
Grid	51.9 ± 1.5	34.0 ± 1.2	13.1 ± 5.5	7.1 ± 3.7
Logistics	67.2 ± 0.3	25.6 ± 1.6	22.7 ± 8.6	9.6 ± 4.4
Rovers	60.5 ± 0.2	24.7 ± 0.2	12.2 ± 3.5	1.9 ± 0.8
Satellite	51.2 ± 0.4	27.5 ± 0.6	1.2 ± 0.4	0.5 ± 0.1
Mean	53.4 ± 13.5	23.2 ± 10.6	9.5 ± 8.4	3.6 ± 3.8

Table 15. Plan-Level Evaluation (BAAI/bge-m3). Trajectory metrics across Interpolation and Extrapolation splits.

Domain	Interpolation		Extrapolation	
	Mean Hit@5	Exact Hit@5	Mean Hit@5	Exact Hit@5
Blocksworld	16.7 ± 0.3	0.3 ± 0.1	0.7 ± 0.3	0.0 ± 0.0
Depot	31.1 ± 1.6	10.8 ± 1.1	2.9 ± 1.2	1.8 ± 1.2
Ferry	60.9 ± 2.0	29.1 ± 2.3	1.2 ± 1.0	0.6 ± 0.5
Floortile	9.2 ± 0.5	3.0 ± 0.4	0.2 ± 0.1	0.1 ± 0.1
Goldminer	26.8 ± 0.8	10.5 ± 0.5	5.1 ± 1.2	1.8 ± 0.3
Grid	32.7 ± 2.7	17.5 ± 2.6	17.6 ± 2.6	7.7 ± 0.9
Logistics	41.3 ± 2.2	9.9 ± 1.9	12.1 ± 5.4	2.4 ± 1.0
Rovers	0.1 ± 0.0	0.0 ± 0.0	—	—
Satellite	0.2 ± 0.1	0.1 ± 0.0	0.0 ± 0.0	0.0 ± 0.0
Mean	24.3 ± 19.5	9.0 ± 9.5	5.0 ± 6.3	1.8 ± 2.5

Table 16. Plan-Level Evaluation (MPNet). Trajectory metrics across Interpolation and Extrapolation splits.

F.2. Domain Complexity Analysis

Correlation analysis reveals moderate positive correlation between average state space size and generalization gap (Pearson $r = 0.42$, $p = 0.26$), though not statistically significant with $n = 9$ domains. Domains with complex multi-object interactions (Depot, Logistics) show larger gaps than domains with simpler dynamics (Goldminer, Grid).

Statistic	Value
Interpolation	$99.5\% \pm 0.6\%$
Extrapolation (Problem-Grouped)	$47.7\% \pm 13.9\%$
Gap	51.8 pp
Paired t -test	$t(8) = 10.58$
p -value	5.57×10^{-6}
95% CI	[40.7, 62.9] pp

Table 17. Statistical analysis of the generalization gap.

Comparison	Δ	Cohen's d	p
Interpolation vs. Extrapolation	-51.8 pp	5.25	$< 10^{-5}$
Extrapolation vs. Cross-Domain	-48.0 pp	4.32	$< 10^{-5}$
Cross-Domain vs. Untrained	+2.7 pp	0.82	0.032
Llama vs. MPNet (Ext.)	+27.8 pp	2.53	< 0.001
Single vs. Multi (Ext.)	+17.4 pp	1.42	0.028

Table 18. Effect sizes for major findings.

G. Ablations

G.1. Architecture and Encoder Comparison

Architecture choice has minimal impact on performance (paired t -test: $p > 0.5$ for all comparisons). The generalization gap is consistent across architectures, confirming that the limitation stems from embedding structure rather than transition network design.

Larger encoders yield better extrapolation performance, but the improvement is sublinear: a $700\times$ increase in parameters (MPNet to Llama) yields only a $2.2\times$ improvement in Hit@5. This suggests that scale alone does not resolve the fundamental structural limitation.

G.2. Effect of Action Disambiguation Loss

We ablate the contribution of the action disambiguation loss $\mathcal{L}_{\text{action}}$ by comparing models trained with the full composite objective ($\lambda = 2$, i.e., $\mathcal{L} = \mathcal{L}_{\text{state}} + 2\mathcal{L}_{\text{action}}$) against models trained with state prediction loss only ($\lambda = 0$).

The action disambiguation loss yields substantial improvements across both metrics and all nine domains. The direct target—Action Acc@5—shows the most dramatic gain, improving $3.4\times$ from 4.8% to 16.2%. Without explicit supervision on action effects, models fail to distinguish between actions with similar but distinct consequences: Action Acc@5 under $\lambda = 0$ barely exceeds the untrained baseline in most domains, indicating that state prediction loss alone provides essentially no signal for learning action semantics.

Critically, Hit@5 also improves by 19.3 pp (+55% relative), despite $\mathcal{L}_{\text{action}}$ not directly optimizing this metric. This substantial indirect benefit reveals that action disambiguation serves as more than auxiliary supervision—it fundamentally shapes how the transition network represents dynamics. We identify two mechanisms: (1) without action-contrastive training, the model exploits spurious correlations between surface-level state-action features and outcomes, which fail to transfer to unseen problems; (2) the action loss forces the network to encode *causal* transformation patterns—understanding that pick-up (A) and pick-up (B) share abstract structure while differing in object binding—enabling compositional generalization.

The improvement is consistent across domains but varies in magnitude. Grid shows the largest absolute gain in Action Acc@5 (+31.3 pp), likely because its spatial action semantics (movement in cardinal directions) are highly distinctive when explicitly supervised. Depot and Rovers show the largest relative Hit@5 gains (+93% and +55%), suggesting that domains with complex multi-object interactions benefit most from learning precise action effects.

We set $\lambda = 2$ to emphasize action disambiguation, reflecting that distinguishing among K domain actions applied to the same state requires finer-grained representations than distinguishing among B random states in a batch. This design choice proves essential: without it, EMBEDPLAN’s extrapolation capability would drop by over one-third, and action understanding

Domain	Gap (pp)	t-statistic	p-value
Depot	73.4	12.87	1.17×10^{-4}
Ferry	63.3	65.49	3.24×10^{-6}
Satellite	59.9	153.39	4.11×10^{-8}
Blocksworld	58.4	5.95	2.70×10^{-3}
Logistics	55.0	4.28	8.28×10^{-3}
Rovers	50.5	20.22	8.90×10^{-6}
Floortile	44.2	3.68	1.57×10^{-2}
Grid	35.9	5.38	2.40×10^{-3}
Goldminer	25.5	3.54	1.13×10^{-2}

Table 19. Independent t-tests comparing Interpolation vs Extrapolation per domain (Qwen2.5-7B).

Domain	Actions	Predicates	Avg States	Gap
Depot	5	8	1,247	73.4
Logistics	6	6	892	55.0
Satellite	5	8	634	59.9
Blocksworld	4	5	423	58.4
Ferry	3	5	312	63.3
Rovers	9	26	1,891	50.5
Floortile	7	10	567	44.2
Grid	5	9	489	35.9
Goldminer	4	7	234	25.5

Table 20. Domain complexity metrics and generalization gaps.

would be nearly absent.

Given the substantial impact of the action disambiguation loss (+19.3 pp Hit@5, +55% relative), we reference this ablation in the main text (Section 3, Training Objective) and report $\lambda = 2$ as the final configuration. The full ablation across $\lambda \in \{0, 0.5, 1, 1.5, 2, 4\}$ confirms $\lambda = 2$ as optimal; performance degrades slightly at $\lambda = 4$ due to over-emphasis on action discrimination at the expense of state prediction.

H. Preliminary Studies

H.1. Latent Distance Alignment

Before learning transition functions, we tested whether pre-trained embeddings already encode planning-relevant structure. If embedding geometry reflects plan costs, one could use simple distance-based heuristics for search without any additional learning.

Hypothesis. We define *Latent Distance Alignment* (LDA) as the property that embedding distance between a state and goal correlates with the number of actions required to reach the goal:

$$\text{LDA} : \quad \text{corr}(d(e_s, e_g), \text{cost}(s, g)) > 0 \quad (34)$$

where e_s and e_g are the embeddings of state s and goal g , $d(\cdot, \cdot)$ is cosine distance, and $\text{cost}(s, g)$ is the optimal plan length from s to g .

Motivation. This hypothesis draws from successes in other domains. CLIP embeddings align images and text such that semantic similarity corresponds to embedding proximity (Radford et al., 2021). Sentence embeddings place entailed sentences closer than contradictions (Reimers & Gurevych, 2019). We test whether similar alignment emerges for planning cost.

Method. For 21,003 state-goal pairs across 9 domains, we computed embedding distances (using all four encoders) and correlated with ground-truth plan costs from A* search.

Encoder	Parameters	MLP	HyperNetwork
Llama-3.3-70B-70B	70B	54.6 \pm 17.0	53.8 \pm 16.5
Qwen2.5-7B	7B	47.7 \pm 14.8	46.2 \pm 15.1
BGE-M3	568M	33.5 \pm 15.6	32.8 \pm 14.9
MPNet	110M	24.4 \pm 17.1	22.8 \pm 17.4

Table 21. Architecture and encoder comparison (Problem-Grouped, Hit@5 %).

Domain	Hit@5 (%)		Action Acc@5 (%)	
	$\lambda=0$	$\lambda=2$	$\lambda=0$	$\lambda=2$
Blocksworld	30.2 \pm 8	49.1 \pm 10	1.8 \pm 0.4	7.9 \pm 2
Depot	13.4 \pm 4	25.9 \pm 6	1.6 \pm 0.3	7.8 \pm 3
Ferry	24.8 \pm 3	40.6 \pm 3	2.5 \pm 0.5	10.3 \pm 2
Floortile	45.3 \pm 14	68.8 \pm 16	8.2 \pm 3	28.3 \pm 15
Goldminer	55.7 \pm 6	76.2 \pm 5	4.9 \pm 1.2	16.5 \pm 2
Grid	52.1 \pm 2	74.9 \pm 1	18.7 \pm 5	50.0 \pm 8
Logistics	31.5 \pm 9	53.7 \pm 10	1.9 \pm 0.6	8.4 \pm 3
Rovers	35.2 \pm 4	54.4 \pm 3	1.7 \pm 0.3	7.1 \pm 0.4
Satellite	29.8 \pm 5	47.5 \pm 6	2.2 \pm 0.5	9.1 \pm 2
Mean	35.3 \pm 13	54.6 \pm 17	4.8 \pm 5	16.2 \pm 14
Δ	+19.3 pp (+55%)		+11.4 pp (3.4 \times)	

 Table 22. **Ablation: Action Disambiguation Loss.** Comparing models trained without ($\lambda=0$) and with ($\lambda=2$) action disambiguation under Extrapolation evaluation (Llama-3.3-70B). The action loss yields substantial gains in both state prediction (+19.3 pp) and action accuracy (3.4 \times).

Result. After controlling for prompt length as a confound, correlations collapsed to near-zero across all encoders. Pre-trained embeddings do not encode planning cost through geometric distance.

Implication. This negative result motivated our transition learning approach: rather than relying on inherent geometry, we explicitly learn how actions transform states in embedding space.

I. Reproducibility

I.1. Code and Data Availability

Will be released upon publication.

I.2. Experimental Reproducibility

- **Random Seeds:** All experiments run with seeds {42, 123, 456}; results report mean \pm standard error.
- **Hardware:** NVIDIA A100 80GB GPU
- **Software:** PyTorch 2.1, CUDA 12.1, Python 3.10

J. Error Analysis

We qualitatively analyzed Hit@5 errors under Extrapolation evaluation to characterize failure modes. Specifically, we sampled 50 incorrect predictions per domain (where the ground-truth next state ranked outside top-5) and manually inspected the retrieved candidates.

Methodology. For each error, we compared the top-1 retrieved state against the ground-truth next state, counting the number of differing predicates and noting whether both states belonged to the same problem instance.

Findings. Across domains, 78% of top-1 errors shared the same problem instance as the query state. Among these, the median predicate difference was 2 (IQR: 1–3). Table 23 shows representative examples.

Domain	Ground Truth s'	Retrieved \hat{s}'
Blocks	Block A is clear, arm holds B, C is on table	Block A is clear, arm holds C, B is on table
Ferry	Car c1 at 10, ferry empty, c2 at 11	Car c1 at 10, ferry empty, c2 at 10
Logistics	Package p1 in truck t0, t0 at 11-0	Package p1 at 11-0, t0 at 11-0

Table 23. Representative Hit@5 errors. Retrieved states differ from ground truth by 1–2 predicates (italicized), typically involving object locations or holdings within the same problem instance.

These errors suggest the model captures coarse transition structure (correct problem context, approximate state region) but struggles to resolve fine-grained predicate changes, particularly when multiple objects undergo similar transformations.

K. Complete Results Tables

See Tables 24 – 25.

Domain	Split	Hit@1	Hit@5	Hit@10
Blocksworld	Interpolation	94.3±0.3	100.0±0.0	100.0±0.0
	Problem-Grouped	14.2±5.7	41.6±12.5	56.6±11.8
Depot	Interpolation	76.7±1.4	98.2±0.2	99.0±0.0
	Problem-Grouped	4.9±1.7	24.8±7.0	42.2±11.0
Ferry	Interpolation	98.7±0.1	99.9±0.0	100.0±0.0
	Problem-Grouped	10.7±1.1	36.7±1.0	52.8±1.5
Floortile	Interpolation	96.2±0.4	99.4±0.0	99.6±0.0
	Problem-Grouped	24.0±8.1	55.2±15.5	69.0±16.2
Goldminer	Interpolation	94.0±0.8	99.9±0.0	100.0±0.0
	Problem-Grouped	34.5±9.6	74.4±8.1	86.7±3.1
Grid	Interpolation	80.9±1.7	98.6±0.1	99.6±0.1
	Problem-Grouped	19.4±4.5	62.7±7.4	76.9±8.0
Logistics	Interpolation	88.9±1.5	99.6±0.1	99.8±0.0
	Problem-Grouped	14.9±6.5	44.7±16.0	60.7±17.4
Rovers	Interpolation	97.4±0.2	99.7±0.0	99.8±0.0
	Problem-Grouped	18.5±1.4	49.2±2.5	65.0±2.6
Satellite	Interpolation	98.1±0.2	99.9±0.0	100.0±0.0
	Problem-Grouped	14.3±0.6	40.0±0.8	54.8±1.4

Table 24. Complete metrics for Qwen2.5-7B across all domains and splits.

Domain	Split	Hit@1	Hit@5	Hit@10
Blocksworld	Interpolation	96.2±0.4	100.0±0.0	100.0±0.0
	Problem-Grouped	17.6±9.0	49.1±17.0	64.6±13.0
Depot	Interpolation	79.5±1.2	98.8±0.1	99.2±0.1
	Problem-Grouped	4.7±2.0	25.9±11.0	41.2±14.0
Ferry	Interpolation	99.1±0.1	100.0±0.0	100.0±0.0
	Problem-Grouped	12.0±3.0	40.6±6.0	58.1±7.0
Floortile	Interpolation	97.4±0.3	99.6±0.0	99.8±0.0
	Problem-Grouped	37.6±22.0	68.8±27.0	78.9±22.0
Goldminer	Interpolation	95.8±0.6	100.0±0.0	100.0±0.0
	Problem-Grouped	35.8±11.0	76.2±9.0	88.0±3.0
Grid	Interpolation	84.3±1.4	99.8±0.0	99.9±0.0
	Problem-Grouped	25.7±2.0	74.9±2.0	88.0±2.0
Logistics	Interpolation	91.2±1.1	99.9±0.0	100.0±0.0
	Problem-Grouped	16.5±6.0	53.7±17.0	70.8±17.0
Rovers	Interpolation	97.8±0.2	99.0±0.1	99.5±0.1
	Problem-Grouped	16.9±2.0	54.4±5.0	72.2±4.0
Satellite	Interpolation	98.5±0.2	99.9±0.0	100.0±0.0
	Problem-Grouped	14.4±4.0	47.5±10.0	66.9±10.0

Table 25. Complete metrics for Llama-3.3-70B-70B across all domains and splits.